Proceedings of the
Annual Stability Conference
Structural Stability Research Council
Toronto, Canada, March 25-28, 2014

A Novel DSM-Based Approach for the Rational Design of Fixed-Ended and Pin-Ended Short-to-Intermediate Angle Columns

P.B. Dinis[1], D. Camotim[1], N. Peres[2]

Abstract

This paper deals with the development of novel procedures for the design of fixed-ended and pin-ended equal-leg angle columns with short-to-intermediate lengths, *i.e.*, those buckling in flexural-torsional modes. Initially, numerical results concerning the buckling and post-buckling behavior of the above angle columns are presented, (i) highlighting the main differences between the fixed-ended and pin-ended column responses, and (ii) evidencing the need for specific design procedures. Then, the paper gathers a large column ultimate strength data bank that includes (i) experimental values, collected from the available literature, and (ii) numerical values, obtained from ABAQUS shell finite element analyses. The set of experimental results collected comprises *41* fixed-ended and *35* pin-ended columns, and the numerical results obtained concern *337* fixed-ended and *197* pin-ended columns – various cross-section dimensions, lengths and yield stresses are considered. Next, after reviewing the available methods to estimate the ultimate strength of angle columns, the paper develops new design approaches for fixed-ended and pin-ended columns, based on the Direct Strength Method (DSM) – the mechanical reasoning behind the procedures proposed, which include the use of genuine flexural-torsional strength curves, is also provided. Finally, the paper closes with the assessment of the ultimate strength predictions yielded by the proposed DSM design procedures, through their comparison with the assembled experimental and numerical failure loads – it is shown that both the quality and reliability of these predictions are very good and slightly higher than those exhibited by the available design methods for angle columns.

1. Introduction

Thin-walled angle columns are known to possess no primary warping resistance (the cross-section warping constant stems exclusively from secondary warping), which implies an extremely low torsional stiffness and, therefore, a high susceptibility to instability phenomena involving torsion, namely flexural-torsional buckling (equal-leg angles are singly symmetric cross-sections). Since the flexural-torsional deformations exhibited by equal-leg angle columns with short-to-intermediate lengths are very similar (akin) to local deformations, these members have been said to fail in "local-global interactive modes", which explains why most of the existing methods for their design are based on local strength concepts/curves. Since column flexural-torsional (global) and local buckling are commonly associated with markedly different post-critical behaviors (strength reserves), the definition of a rational (structurally well founded) design

[1] Civil Engineering Department, ICIST, Instituto Superior Técnico, Technical University of Lisbon, Portugal. <dinis; dcamotim@civil.ist.utl.pt>
[2] Civil Engineering Department, Universidade Nova de Lisboa (FCT/UNL), Portugal. < nr.peres@campus.fct.unl.pt>

model/procedure to provide accurate ultimate strength estimates for thin-walled equal-leg angle columns must necessarily involve flexural-torsional strength concepts/curves (instead of local ones).

The post-buckling behavior, strength and design of angle columns has attracted the attention of several researchers in the past (*e.g.*, Kitipornchai & Chan 1987, Kitipornchai *et al.* 1990, Popovic *et al.* 1999, Young 2004, Ellobody & Young 2005, Rasmussen 2005, 2006, Chodraui *et al.* 2006, Maia *et al.* 2008, Shifferaw & Schafer 2011, and Mesacasa Jr. 2012). Nevertheless, numerical simulations recently carried out by the authors (Dinis & Camotim 2011, Dinis *et al.* 2012), concerning pin-ended (but with end-section warping prevented) and fixed-ended short-to-intermediate equal-leg angle columns, shed new light on key (and somewhat surprising) mechanical aspects related with the structural response of such members, namely the fact that it is strongly influenced by the interaction between two global buckling modes (one involving major-axis flexure and torsion, and the other minor-axis flexure only)[3]. They also showed that a single design approach cannot handle adequately both pin-ended and fixed-ended angle columns – this is because, due to the effective centoid shift (*e.g.*, Young & Rasmussen 1999), the mode interaction effects are much more relevant in the former case. These findings led Dinis *et al.* (2010a, 2011) and Silvestre *et al.* (2013) to propose different design approaches for pin-ended and fixed-ended columns, both based on the Direct Strength Method (DSM – *e.g.*, Schafer 2008), which combine (i) the experimentally-based global design curve proposed by Young (2004) with (ii) either the current DSM local strength curve (fixed-ended columns) or an empirically determined lower "local" design curve (pin-ended columns). Although these DSM-based design approaches were shown (i) to provide efficient (accurate and reliable) estimates of the available pin-ended and fixed-ended experimental and numerical failure loads, and (ii) to outperform all their predecessors, they exhibit one non-negligible drawback: the lack of an underlying rational structural model. This is mainly because they do not take into account explicitly the fact that the column behavior and failure are governed by the interaction between minor-axis flexural and major-axis flexural-torsional (instead of local) buckling effects, which are markedly different for pin-ended and fixed-ended equal-leg columns (Dinis *et al.* 2012).

Last year, Dinis *et al.* (2013) contributed to overcome the above limitation by proposing more rational DSM-based design approaches for fixed and pinned equal-leg angle columns. The key contribution consisted of retaining the current DSM global strength curve, while replacing the local curve by a set of genuine flexural-torsional curves that were specifically developed for equal-leg angle columns and, thus, account for the structural peculiarity of this cross-section shape (note that it is formed by just two outstands, which renders the mode interaction effects remarkably relevant – particularly in the pin-ended columns, due to the effective centroid shift). Moreover, it was also clearly shown that (i) both the column post-buckling behavior and effective centroid shift effects are length-dependent (the latter only in pin-ended columns), and that (ii) this length-dependence is linked to the column critical buckling mode characteristics, namely the amount of major-axis flexure. The above findings were used to propose and provide preliminary illustration of a methodology for the development of a unified and rational DSM-based approach to predict the failure loads of fixed-ended and pin-ended (with cylindrical supports) short-to-intermediate equal-leg angle columns.

This paper provides the closure for work described in the previous paragraph, in the sense that presents the development, illustrates the application and assesses the quality of a novel DSM-based approach for the rational design of fixed-ended and pin-ended short-to-intermediate equal-leg angle columns subjected

[3] This interaction was very recently investigated in some detail by Mesacasa Jr. *et al.* (2013).

to uniform compression[4]. Initially, numerical results concerning the angle column buckling and post-buckling behavior are presented, (i) highlighting the differences between the fixed-ended and pin-ended (cylindrical supports) column responses, and (ii) evidencing the need for specific design procedures. Then, the paper gathers a large column failure load data bank that includes (i) *76* experimental values (*41* fixed-ended and *35* pin-ended specimens), collected from the literature, and (ii) *534* numerical values (*337* fixed-ended and *197* pin-ended columns), yielded by ABAQUS shell finite element analyses (SFEA) – various cross-section dimensions, lengths and yield stresses are considered. Then, after reviewing the most efficient DSM-based design methodologies available to estimate the ultimate strength of equal-leg angle columns (against "local"-global failures), the paper presents the development of the aforementioned novel DSM-based design approach for fixed-ended and pin-ended columns, including the mechanical reasoning behind the procedures proposed. Following a careful calibration procedure, the selections of the appropriate flexural-torsional strength curves (post-buckling behavior) and erosion coefficients (effective centroid shift effects) are presented – they are expressed on the sole basis of the column torsional and flexural-torsional critical buckling loads. Finally, the quality of the ultimate strength predictions provided by the novel DSM design procedures is assessed, through the comparison with the gathered experimental and numerical failure load data bank – both the quality and reliability of these predictions are shown to be very good and, moreover, higher than those exhibited by the best available design methods for angle columns, namely those proposed by Young (2004), Rasmussen (2006) and Silvestre *et al.* (2013).

2. Buckling and Post-Buckling Behavior

The peculiar behavioral features exhibited by angle columns are briefly addressed in this section – more information can be found in Dinis *et al.* (2010a,b, 2011, 2012, 2013) and Dinis & Camotim (2011). Particular attention is paid to the issues having higher impact on the development of the DSM design approach dealt with in this work. The columns analyzed exhibit (i) pinned (cylindrical supports with the secondary warping prevented) or fixed end sections, (ii) equal legs (*70×70 mm* and *t=1.2mm* – the effect of rounded corners is disregarded) and (iii) short-to-intermediate lengths. Almost all the numerical results were obtained through ABAQUS (Simulia 2008) shell finite element analyses, (i) adopting column discretizations into fine 4-node isoparametric element meshes (length-to-width ratio close to *1*) and (ii) modeling the column supports by (ii_1) fully attaching rigid end-plates to the member end sections (thus ensuring the secondary warping and local displacement/rotation restraints) and (ii_2) preventing both the major and minor-axis flexural rotations (fixed supports – F condition) or only the major-axis flexural rotations (pinned supports with cylindrical hinges – P condition[5]) – the torsional rotations are prevented in both cases. However, in order to characterize and distinguish between local and global buckling of angle columns, GBT analyses are also performed using the code GBTUL (Bebiano *et al.* 2008a,b).

2.1 Buckling Behavior

The curves shown in Fig. 1(a), obtained through GBTUL and ABAQUS SFE analyses, provide the variation of P_{cr} (critical load) with the length L (logarithmic scale), both for F and P columns – the GBT analyses included *7* deformation modes: *4* global (**1**-**4**) and *3* local (**5**-**7**). As for Fig. 1(b), it displays the GBT F and P column modal participation diagrams – they provide the contributions of each GBT deformation

[4] Naturally, there is considerable overlap between the content of this paper and that of its predecessor (Dinis *et al.* 2013). This is because, for the sake of cmpletion and better readability, it was decided to include here all the material that is relevant for the developemnt of the DSM-based rational design approach under consideration. In other words, this paper should be viewed as the "final version" of work initiated last year (Dinis *et al.* 2013 was the "preliminary version").

[5] These are the end support conditions adopted in the "pin-ended angle column experimental tests" reported in the literature.

mode to the column critical buckling modes (Dinis *et al.* 2010b). Finally, Fig. 1(c) shows the buckling modes of P columns with $L=100,364,1000cm$, as well as the in-plane shapes of *6* (out of 7) deformation modes considered (axial extension not shown). These buckling results prompt the following remarks:

(i) The "plateau" in the P_{cr} vs. L curve corresponds to flexural-torsional buckling, as the column buckling modes combine participations from deformation modes **4** (torsion) and **2** (major-axis flexure). Moreover, the amount of major axis flexure is initially minute and becomes increasingly visible as L increases – in order to enable a quantification of the percentage participation of mode **2** in the column buckling mode (p_2), the table in Fig. 1(b) shows its variation with L.

(ii) The P columns only differ from their F counterparts in the smaller length range associated with the "plateau", due to the *75%* drop in the minor-axis flexural buckling loads – the transition from flexural-torsional buckling to minor-axis flexural (mode **3**) buckling occurs for either $L=420cm$ (P columns) or $L=890cm$ (F columns). For lengths below $L=420cm$, the P and F column local and flexural-torsional buckling loads and mode shapes are identical.

(iii) In order to assess how the column post-buckling behavior varies as one progresses along the P_{cr} *vs.* L curve "plateau", the following lengths are selected (see Fig. 1(a)): $L_1=53cm$, $L_2=133cm$, $L_3=364cm$ and $L_4=700cm$ – *4* F (F_1-F_4 – $22.1\leq f_{cr}\leq 27.5MPa$) and *3* P ($P_1$-$P_3$ – $23.4\leq f_{cr}\leq 27.5MPa$) columns.

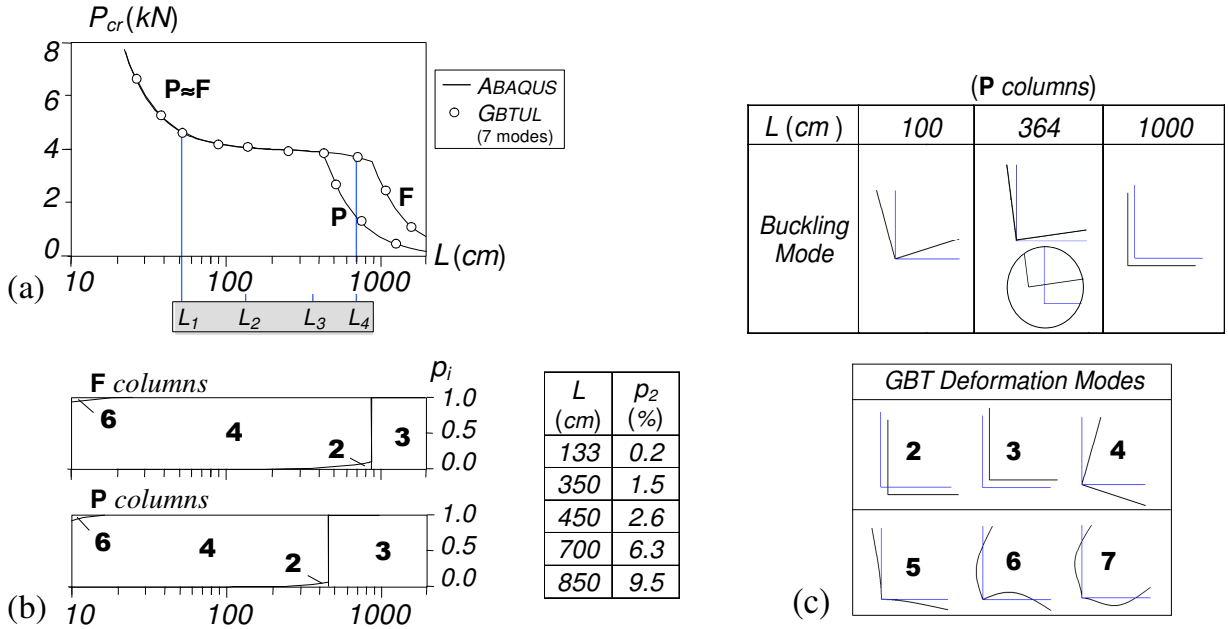

Figure 1: (a) P_{cr} vs. L curves and (b) GBT modal participation diagrams (F and P columns), including a table with a few p_2 values, and (c) in-plane shapes of *3* buckling modes and first *6* GBT deformations modes (P columns)

2.2 Elastic-Plastic Post-Buckling Behavior

The elastic-plastic behavior and strength of F and P short-to-intermediate angle columns is addressed next. The results concern columns (i) containing critical-mode initial imperfections with *0.1t* amplitude and (ii) exhibiting *4* yield-to-critical stress ratios: $f_y/f_{cr}\approx 1.3,2.5,5.0$ and ∞, concerning $f_y=30,60,120MPa$ and elastic behavior ("average" $f_{cr}=24MPa$) – some unrealistically low yield stresses are considered, in order to cover a wide slenderness range.

Figs. 2(a)-(b) show the upper parts ($P/P_{cr}>0.6$) of the elastic equilibrium paths P/P_{cr} vs. β (β is the mid-span web chord rigid-body rotation) for the F_1-F_4 (Fig. 2(a)) and P_1-P_3 (Fig. 2(b)) columns – additional

information can be found in Dinis *et al.* (2012). After observing these results, it is readily concluded that the angle column post-buckling is highly length-dependent within the $P_{cr}(L)$ curve plateau (see Fig. 1(a)). While the shorter columns exhibit substantial post-critical strength and little minor-axis flexure, the longer ones have minute post-buckling strength and considerable minor-axis flexure. The amount of major-axis flexure appearing in the column critical buckling mode (see Fig. 1(b)) was found to increase along the $P_{cr}(L)$ curve plateau and correlate quite well with its post-buckling strength.

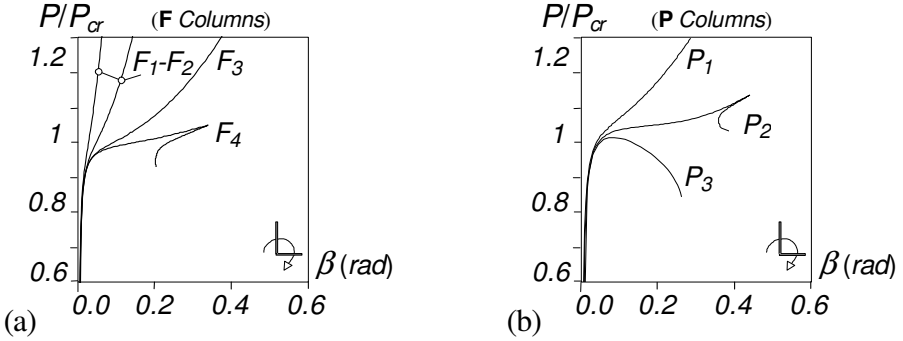

Figure 2: P/P_{cr} *vs.* β equilibrium paths: (a) F_1-F_4 and (b) P_1-P_3 columns

Fig. 3(a) depicts typical short F column elastic-plastic equilibrium paths: the upper parts ($P/P_{cr}>0.5$) of the F_3 column P/P_{cr} vs. β paths for yield-to-critical stress ratios $f_y/f_{cr}\approx 1.3, 2.5, 5.0$ (and also the elastic path, already shown in Fig. 2(a)) – this figure also displays the plastic strain diagram at collapse for $f_y/f_{cr}\approx 2.5$. As for Fig. 3(b), it concerns a longer F column elastic-plastic post-buckling behavior: upper parts of the F_4 column P/P_{cr} vs. β paths for the above four f_y/f_{cr} values and also the $f_y/f_{cr}\approx 2.5$ column (elastic) collapse mechanism. The observation of all these results leads to the following remarks:

(i) While the F_3 columns with $f_y/f_{cr}\approx 1.3$, 2.5 fail at the onset of yielding, their $f_y/f_{cr}\approx 5.0$ counterpart exhibits a very small elastic-plastic strength reserve. The F_3 column ultimate load grows visibly with f_y – *e.g.*, an increase from *30* to *120MPa* more than doubles the load-carrying capacity.

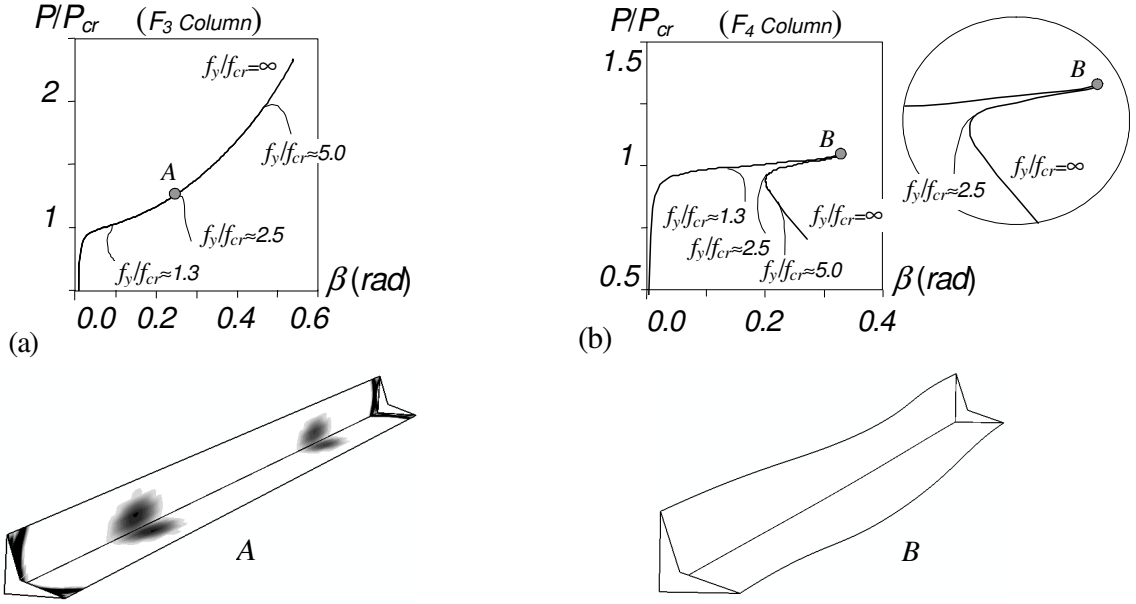

Figure 3: P/P_{cr} vs. β equilibrium paths ($f_y/f_{cr}\approx 1.3, 2.5, 5.0$) and failure mechanism ($f_y/f_{cr}\approx 2.5$) for the (a) F_3 and (b) F_4 columns

(ii) The plastic strain diagram *A* in Fig. 3(a) shows that, in the F_3 columns, yielding occurs around the one and three quarter-span zones of the internal longitudinal edge, where the shear and longitudinal normal stresses, due to the torsional rotation variation, are higher (Stowell 1951, Dinis *et al.* 2012).

(iii) The F_4 column ultimate strength is practically insensitive to f_y, as the collapse is predominantly due to geometrically non-linear effects. Indeed, for $f_y/f_{cr} \approx 2.5, 5.0$ the column remains elastic up until failure, as the onset of yielding only takes place well inside the equilibrium path descending branch.

A similar investigation was performed for the P columns and Fig. 4 displays (i) the upper parts ($P/P_{cr} > 0.5$) of the P/P_{cr} *vs.* β paths for P_2 columns with $f_y/f_{cr} \approx 1.3, 2.5, 5.0, \infty$, and (ii) the plastic strain diagram at collapse associated with $f_y/f_{cr} \approx 2.5$. The observation of these post-buckling results shows that:

(i) There is virtually no elastic-plastic strength reserve or ductility prior to failure – yielding starts in the middle of the vertical leg at the one and three quarter-span cross-section, and precipitates failure.

(ii) There is a rather small variation of the column ultimate load with the yield stress – *e.g.*, a rise from *30* to *120 MPa* entails a small failure load increase (only *9.4%*). Moreover, there is no benefit in increasing the yield stress beyond five times f_{cr}, since for $f_y/f_{cr} \approx 5.0$ the collapse occurs, abruptly, in the elastic range (the $f_y/f_{cr} \approx 5.0$ and $f_y/f_{cr} \approx \infty$ curves share the same limit point).

(iii) The above P_2 column post-buckling behavioral features are also exhibited, to an even larger extent, by the longer P columns, such as the P_3 one – recall its elastic post-buckling equilibrium paths, shown in Fig. 2(b), which display smooth limit points for $P/P_{cr} \approx 1.0$.

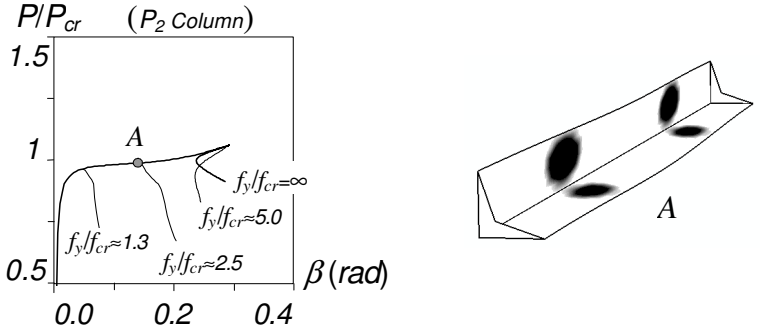

Figure 4: P_2 column elastic-plastic post-buckling behavior: P/P_{cr} vs. β equilibrium paths ($f_y/f_{cr} \approx 1.3, 2.5, 5.0$) and plastic strain diagram and failure mode ($f_y/f_{cr} \approx 2.5$)

The markedly different elastic and elastic-plastic post-buckling behaviors displayed by the F and P short-to-intermediate equal-leg angle columns implies that there is a significant discrepancy between their ultimate strengths P_u associated with a given yield stress. Since all these columns have virtually identical critical stresses, thus sharing a common critical slenderness $\lambda = (P_y/P_{cr})^{0.5}$, their P_u/P_y values may exhibit a high "vertical dispersion" with respect to λ – this behavioral feature must be adequately taken into account by an efficient design procedure for equal-leg angle columns.

3. Failure Load Data: Test Results and Numerical Simulations

Following the findings reported by Dinis *et al.* (2010a, 2011, 2012) and Dinis & Camotim (2011), which were summarized above, Silvestre *et al.* (2013) decided to assess the performance of the then existing design rules for cold-formed steel equal-leg angle columns with short-to-intermediate lengths. This task required the assembly a fairly large column ultimate strength data bank, comprising (i) experimental failure loads reported in literature and (ii) numerical failure loads determined by means of ABAQUS SFEA (employing the model developed earlier, also used to obtain the results presented in the previous section).

The experimental failure loads concern (i) *41* fixed-ended columns, tested by Popovic *et al.* (1999), Young (2004) and Mesacasa Jr. (2012)[6], and (ii) *35* pin-ended columns (with cylindrical supports), tested by Wilhoite *et al.* (1984), Popovic *et al.* (1999), Chodraui *et al.* (2006) and Maia *et al.* (2008). The specimen cross-section geometries, lengths L, yield stresses f_y and ultimate stresses f_u are given in Annexes B (F columns) and C (P columns). Detailed accounts of these experimental investigations can be found in the above publications – see also the overview provided by Silvestre *et al.* (2013).

The numerical (SFEA) failure loads concern (i) *337* fixed-ended and (ii) *197* pin-ended columns, exhibiting (i) *6* cross-section dimensions (*50×1.2mm*, *50×2.6mm*, *60×1.5mm*, *70×1.2mm, 70×2.0mm* and *90×2.5mm*), (ii) lengths selected to ensure critical flexural-torsional modes buckling (*i.e.*, all columns fall within the P_{cr} vs. L curve "horizontal plateaus" shown in Fig. 1(a)) and (iii) yield stresses chosen to enable covering a wide critical slenderness range. The column cross-section geometries, selected lengths L, adopted yield stresses f_y and obtained ultimate stresses f_u are given in Annexes D (F columns) and E (P columns). It is worth noting that part of the F and P column results shown here had already been reported by Silvestre *et al.* (2013) – the remaining ones, freshly determined in the course of this study, concern (i) F columns with (i_1) *60×1.5mm* and *L=800*,*900*,*1000*,*1500*,*2000*,*2500*,*3000*,*3500*,*4000*, *4500*,*5000*,*5260mm*, (i_2) *70×2.0mm* and *L=700*,*800*,*900*,*1000*,*1500*,*2000*,*2500*,*3000*,*3500*,*4000*,*4500*, *5000*,*5360mm*, and (i_3) *90×2.5mm* and *L=1000*,*1200*,*1500*,*2000*,*2500*,*3000*,*4000*,*5000*, *6000*,*7000mm*, and (ii) P columns with (ii_1) *50×1.2mm* and *L=750*,*950*,*1500*,*2000mm*, (ii_2) *60×1.5mm* and *L=800*,*900*, *1000*,*1500*,*2000*,*2500mm*, (ii_3) *50×2.6mm* and *L=750*,*950mm*, (ii_4) *70×2.0mm* and *L=700*,*800*,*900*, *1000*,*1500*,*2000*,*2500mm*, and (ii_5) *90×2.5mm* and *L=1000*,*1200*,*1500*,*2000*,*2500*,*3000mm*. In all the analyses, the steel material behavior was modeled as elastic-perfectly plastic (*E=210GPa*, *ν=0.3*) and both residual stresses and rounded corner effects are disregarded. Preliminary numerical studies showed that the combined influence of strain hardening, residual stresses and rounded corner effects has little impact on the angle column failure loads (all differences below *3%*), which is in line with the findings reported by other authors, namely Ellobody & Young (2005) and Shi *et al.* (2009). As mentioned earlier, the yield stresses f_y were selected to cover a wide critical slenderness range, which implied considering a few unrealistic (small or large) values – the yield stress values adopted were (i) *30*,*60*,*120*,*235*,*400*, *500MPa* (*70×1.2mm* columns), (ii) *120*,*235*,*400*,*500MPa* (*50×1.2mm* and *50×2.6mm* columns), and (iii) *120*,*235*,*400*,*500*,*600*,*900*,*1200MPa* (*60×1.5mm*, *70×2.0mm* and *90×2.5mm* columns).

Following the behavior observed in the experimentally tested columns, namely the length-dependency of the imperfection-sensitivity, a preliminary study was carried out to identify the most detrimental imperfection shape – critical flexural-torsional and/or minor-axis flexural shape. Although the columns with shorter lengths (left and central zones of the $P_{cr}(L)$ curve horizontal plateaus) were found to be virtually insensitive to the minor-axis flexural imperfections (only the flexural-torsional imperfections are relevant)[7], it was decided to determine, for all F and P columns analyzed, failure loads stemming from the simultaneous presence of flexural-torsional and minor-axis flexural initial geometrical imperfections – the columns contained initial imperfections combining (i) a critical flexural-torsional component, with amplitude equal to *10%* of the wall thickness t, and (ii) a non-critical minor-axis flexural component, with

[6] Four tests reported by Maia *et al.* (2008) were excluded from this study, since the ultimate strengths reported are much lower than the numerical results obtained by the same authors, adopting moderate-to-high torsional initial imperfections (*0.64t* and *1.55t*). In the authors' opinion, these fixed-ended columns contained abnormally large initial imperfections and/or load eccentricities (possibly caused by the procedure adopted to ensure the column end section fixity).

[7] A detailed investigation on the imperfection-sensitivity, associated with the simultaneous presence of flexural-torsional and minor-axis flexural initial imperfections, of equal-leg angle columns was very recently reported by Mesacasa Jr. *et al.* (2013).

amplitude equal to *L/750* (F columns) or *L/1000* (P columns)[8] – values in line with the measurements reported for the column specimens tested by Young (2004) and Popovic *et al.* (1999), respectively.

4. Direct Strength Method (DSM) Design

The current DSM strength/design curves for cold-formed steel columns are defined by "Winter-type" expressions that (i) were calibrated against fairly large numbers of experimental and/or numerical results and (ii) provide safe and accurate ultimate strength estimates associated with local, distortional, global and local-global interactive failures on the sole basis of elastic critical buckling (f_{crl}, f_{crd}, f_{cre}) and yield stresses (*e.g.*, Schafer 2008). In the context of this investigation on angle columns, not (yet) pre-qualified for the DSM design, the relevant nominal strengths are f_{nl} (local), f_{ne} (global) and f_{nle} (local-global), given by

$$f_{nl} = \begin{cases} f_y & \text{if} \quad \lambda_l \le 0.776 \\ f_y \left(\frac{f_{crl}}{f_y} \right)^{0.4} \left[1 - 0.15 \left(\frac{f_{crl}}{f_y} \right)^{0.4} \right] & \text{if} \quad \lambda_l > 0.776 \end{cases} \quad \text{with} \quad \lambda_l = \sqrt{\frac{f_y}{f_{crl}}} \quad , \quad (1)$$

$$f_{ne} = \begin{cases} f_y \left(0.658^{\lambda_c^2} \right) & \text{if} \quad \lambda_c \le 1.5 \\ f_y \left(\frac{0.877}{\lambda_c^2} \right) & \text{if} \quad \lambda_c > 1.5 \end{cases} \quad \text{with} \quad \lambda_c = \sqrt{\frac{f_y}{f_{cre}}} \quad , \quad (2)$$

$$f_{nle} = \begin{cases} f_{ne} & \text{if} \quad \lambda_{le} \le 0.776 \\ f_{ne} \left(\frac{f_{crl}}{f_{ne}} \right)^{0.4} \left[1 - 0.15 \left(\frac{f_{crl}}{f_{ne}} \right)^{0.4} \right] & \text{if} \quad \lambda_{le} > 0.776 \end{cases} \quad \text{with} \quad \lambda_{le} = \sqrt{\frac{f_{ne}}{f_{crl}}} \quad . \quad (3)$$

Since local and torsional deformations are akin in angle columns, (i) both designations are often used indistinctly in the context of these columns and (ii) f_{nle} expressions are commonly used to estimate their "local"-global failure loads – however, such an approach neglects the fact that angle columns effectively buckle in flexural-torsional modes and, moreover, that the mechanical characteristics of these flexural-torsional modes vary significantly along the $P_{cr}(L)$ curve horizontal plateau.

The most relevant design proposals for angle columns were recently revised by Silvestre *et al.* (2013) and Dinis *et al.* (2013), namely those proposed by Young (2004) and Rasmussen (2006). The latter developed a DSM-based approach for the design of P angle columns that incorporates explicitly the eccentricity stemming from the effective centroid shift – the strength curve depends on λ_l, reads

$$f_{nl} = \rho \cdot \beta \cdot f_y \quad , \quad (4a)$$

$$\rho = \frac{A_e}{A} = \begin{cases} 1 & \text{if} \quad \lambda_l \le 0.673 \\ \frac{\lambda_l - 0.22}{\lambda_l^2} & \text{if} \quad \lambda_l > 0.673 \end{cases} \quad , \quad (4b)$$

$$\beta = \begin{cases} 1 & \text{if} \quad \lambda_l \le 1.22 \\ \frac{0.68}{(\lambda_l - 1)^{0.25}} & \text{if} \quad \lambda_l > 1.22 \end{cases} \quad , \quad (4c)$$

[8] The initial corner displacements caused by minor-axis flexure values always "point" towards the cross-section corner, thus reinforcing the effective centroid shift effects.

and accounts simultaneously for both the (i) bending effects due to the effective centroid shift, through parameter β, and (ii) "local" (flexural-torsional) buckling effects, through the effective area reduction factor ρ. Moreover, Silvestre *et al* (2013) proposed different DSM-based design approaches for P and F columns, which combine (i) Young's (2004) experimentally-based global design curve with (ii) either the current DSM local strength curve (F columns) or an empirically modified/lowered alternative curve (P columns) – these curves are expressed by

$$f_{ne} = \begin{cases} f_y \left(0.5^{\lambda_c^2}\right) & if \quad \lambda_c \leq 1.4 \\ f_y \left(\dfrac{0.5}{\lambda_c^2}\right) & if \quad \lambda_c > 1.4 \end{cases} \qquad \text{with} \qquad \lambda_c = \sqrt{\frac{f_y}{f_{cre}}} \qquad , \quad (5)$$

$$f_{nl} = \begin{cases} f_y & if \quad \lambda_l \leq 0.71 \\ f_y \left(\dfrac{f_{crl}}{f_y}\right)\left[1 - 0.25\left(\dfrac{f_{crl}}{f_y}\right)\right] & if \quad \lambda_l > 0.71 \end{cases} \qquad \text{with} \qquad \lambda_l = \sqrt{\frac{f_y}{f_{crl}}} \qquad . \quad (6)$$

These DSM-based design approaches were shown (i) to provide safe, accurate and reliable estimates of the then available experimental and numerical failure loads, and, moreover, (ii) to outperform their most efficient predecessors: those developed by Young (2004 – F columns) and Rasmussen (2006 – P columns). The experimental and numerical failure-to-predicted load ratios are given in Annexes B-E[9] – their averages, standard deviations and maximum/minimum values are summarized in Table 1. However, in spite of the quite positive performance indicators, one negative feature subsisted: the lack of a rational structural reasoning, as reflected in (i) the almost fully empirical roots of the strength curves defined by Eqs. (5) and (6), and (ii) the inadequate nature of the only current DSM design curve involved in the approach, which predicts local failure loads (instead of flexural-torsional ones).

Table 1: Means, standard deviations and maximum/minimum values of the experimental and numerical F and P column failure-to-predicted load ratios concerning the design proposals of Young (2004), Rasmussen (2006) and Silvestre *et al.* (2013)

	F Columns				P Columns			
	Young (2004)		Silvestre *et al*. (2013)		Rasmussen (2006)		Silvestre *et al*. (2013)	
	Exp	Num	Exp	Num	Exp	Num	Exp	Num
Mean	1.14	1.14	0.98	1.02	1.09	1.01	1.12	1.10
Sd. Dev.	0.18	0.16	0.15	0.11	0.24	0.09	0.25	0.11
Max	1.70	1.61	1.24	1.40	1.81	1.39	1.89	1.74
Min	0.83	0.95	0.74	0.73	0.72	0.81	0.88	0.96

The next section addresses the development and assessment of novel DSM-based design approaches for F and P equal-leg short-to-intermediate angle columns, which not only (i) share (or even improve) the positive performance indicators exhibited by the approaches proposed by Silvestre *et al.* (2013), but also (ii) are founded on a structural reasoning closely and clearly linked to behavioral features exhibited by the angle columns (*i.e.*, amply deserve to be termed "rational") – the work presented consists of an improvement (refinement is probably a better word) of a preliminary attempt to achieve the above goal, which was very recently reported by Dinis *et al.* (2013).

[9] To obtain the failure load predictions, it was necessary to calculate f_{crft} and f_{cre} for all columns – while the latter can be calculated straightforwardly, the calculation of the former can be performed by means of the analytical expressions derived in Annex A – the corresponding values are given in Annexes B-E.

5. Novel DSM-Based Rational Design Approaches

As shown before, the ultimate strength of both the F and P columns is strongly affected by the "location" of the column length within the $P_{cr}(L)$ plateau, which can be quantified by either (i) the "closeness" between the f_{crft} and f_{cre} values or (ii) the percentage participation of major-axis flexure in the flexural-torsional buckling mode (see the p_2 table in Fig. 1(b)). The shorter columns, located on the left side of the plateau, exhibit (i) clearly stable post-critical behaviors, (ii) very little minor-axis flexure and (iii) very small (virtually imperceptible) p_2 values. Conversely, the longer columns, located on the right side of the plateau, exhibit (i) a minute/negligible post-buckling strength, (ii) considerable minor-axis flexure and (iii) visible (even if fairly small) p_2 values. Therefore, it may be concluded that the column failure load decreases with the length, due to a combination of (i) lower flexural-torsional post-critical strengths, "measured" by p_2, and (ii) higher interaction effects, "measured" by the difference between f_{crft} and f_{cre} – in the P columns, these interaction effects are further enhanced by the effective centroid shifts.

In order to develop rational DSM-based design approaches for F and P angle columns, it is indispensable that they reflect the behavioral features unveiled by Dinis *et al.* (2012) and outlined in section 2. Therefore, it may be established, at the outset, that the sought DSM-based design approaches must exhibit the following characteristics:

(i) Since the intermediate angle columns fail mostly in interactive modes combining flexural (minor-axis) and torsional or flexural-torsional (major-axis) deformations, the strength curves involved must be (i_1) the current DSM global strength curve and (i_2) flexural-torsional strength curves, which need to be developed to replace the single local strength curve in the current DSM design against local-global interactive failures.

(ii) Several flexural-torsional curves must be developed, in order to enable capturing the progressive (length-dependent) erosion of the column post-critical strength as its length increases within the $P_{cr}(L)$ curve plateau – see Figs. 1(a) and 2.

(iii) The effective centroid shift effects, strongly influencing the P angle column failure loads (not the F column ones), must be incorporated into the design approach through a procedure or parameter that only comes into play for the P columns – exactly the idea put forward by Rasmussen (2006) (see the parameter β in Eq. (4c)). However, such procedure/parameter must reflect, as closely as possible, the length-dependence of the column flexural-torsional behavior – note that Rasmussen based his β parameter on local buckling concepts.

Then, the first step towards reaching more rational DSM design approaches for angle columns consists of developing a set of genuine flexural-torsional strength curves covering adequately the whole $P_{cr}(L)$ curve plateau – naturally, such apply to both F and P columns, since their flexural-torsional behaviors are identical. Once this set of flexural-torsional strength curves is determined, it will be possible to propose and assess the merits of a DSM design approach for F angle columns. The same can only be achieved for P angle columns after a quantification of the effective centroid shift effects has been found. This will be done through a "reduction factor" based on the relation between the elastic post-buckling strengths of otherwise identical P and F columns (with and without effective centroid shift effects, respectively).

5.1 Flexural-Torsional Strength Curves

A fully numerical approach is adopted to obtain a set of "Winter-type" strength curves intended to predict, as accurately as possible, "pure flexural-torsional failures" of equal-leg angle columns buckling in flexural-torsional modes. The first step consists of determining a fairly large flexural-torsional failure load data bank, which will be subsequently used to develop and validate the sought strength curves. This is

done by determining the failure loads of *170* columns continuously restrained against minor-axis flexure, *i.e.*, "forced" to fail in a combination of major-axis flexure and torsion. All the columns analyzed are fixed-ended[10] and exhibit (i) three cross-sections (*70×1.2mm*, *50×1.2mm*, *50×2.6mm*), (ii) various lengths (all falling inside the $P_{cr}(L)$ curve plateau), (iii) critical-mode initial imperfections with amplitude equal to *L/1000* and (iv) a large number of yield stress (f_y) values, ranging from *30* to *2200MPa* and selected to ensure covering a wide flexural-torsional slenderness (λ_{ft}) range. Fig. 5(a) plots the obtained ultimate strength ratios f_u/f_y against the column flexural-torsional slenderness λ_{ft} – also depicted in this figure is the current DSM local strength curve. The observation of these results prompts the following remarks:

(i) There is no noticeable difference concerning the f_u/f_y values associated with the three cross-sections considered – the corresponding "f_u/f_y clouds" are virtually identical.

(ii) The huge "vertical dispersion" of the f_u/f_y values makes it easy to conclude that there is no single Winter-type curve that can predict safely and accurately all of them. Moreover, it is also clear that a large number of those values fall well below the current DSM local strength curve, which means that the corresponding failure loads are considerably overestimated by this curve.

(iii) The above "vertical dispersion" is linked to the column length. Indeed, regardless of the particular cross-section considered, the f_u/f_y values gradually decrease as the column length increases (along the $P_{cr}(L)$ curve plateau), which is in line with the findings reported in section 2 (for unrestrained columns). Moreover, it was also found that, regardless of the cross-section geometry once more, the restrained column post-buckling strength consistently decreases as its length progresses along the $P_{cr}(L)$ curve plateau – Fig. 5(b) illustrates this assertion by showing the elastic equilibrium paths of four *70×1.2mm* restrained columns with increasing lengths.

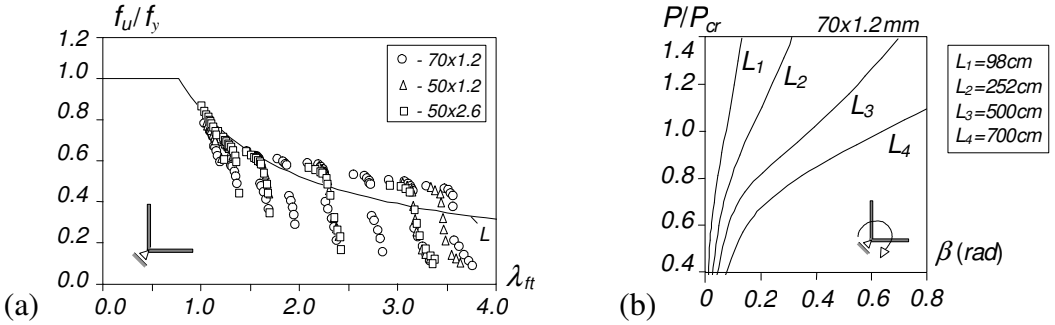

Figure 5: (a) Plot of the column flexural-torsional ultimate strength ratios f_u/f_y against λ_{ft} and (b) elastic equilibrium paths P/P_{cr} vs. β of *70×1.2mm* restrained columns with lengths L=*98*; *252*; *500*; *700cm*

Taking into account the above findings and noting that the GBT modal participation diagrams presented in Fig. 1(b) show that the participation of major-axis flexure (mode **2**) in the column critical (flexural-torsional) buckling mode also increases with the length, it was decided:

(i) To group the columns according to the ratio between their pure torsional (f_{bt}) and flexural-torsional (f_{crft} – critical) buckling stresses, which is directly linked to the participation of mode **2**. These two buckling stresses may be calculated through the analytical formulae derived in Annex A specifically for fixed-ended equal-leg (width b, thickness t, length L) steel (E, $G=E/(2(1+\nu))$) angle columns,

$$f_{bt} = G\frac{t^2}{b^2} + \pi^2 \frac{E\,t^2}{12(L/2)^2} \quad , \qquad (7)$$

[10] Recall that the pin-ended columns restrained against minor-axis flexure are a subset of their fixed-ended counterparts.

$$f_{crft} = \frac{4}{5}\left(f_{bt} + f_{bf} - \sqrt{(f_{bt} + f_{bf})^2 - 2.5\, f_{bt}\, f_{bf}} \right) \quad , \qquad (8)$$

where $f_{bf} = \pi^2 E b^2/(6\,(L/2)^2)$ is the angle column pure major-axis flexural buckling stress – most of the buckling stress values calculated with the above expressions are given in the tables presented in Annexes B-E. Figs. 6(a)-(c) plot f_u/f_y against λ_{ft} for the columns analyzed earlier and sharing similar f_{bt}/f_{crft} ratios, namely 1.0016 (Fig. 6(a)), 1.020 (Fig. 6(b)) and 1.070 (Fig. 6(c)), corresponding to column lengths located on the left side (almost pure torsional buckling), middle and right side of the $P_{cr}\,(L)$ curve plateau. It is observed that, regardless of the cross-section geometry, the f_u/f_y values concerning columns with close f_{bt}/f_{crft} ratios are reasonably well aligned along Winter-type curves, *i.e.*, the "vertical dispersion" is fairly small.

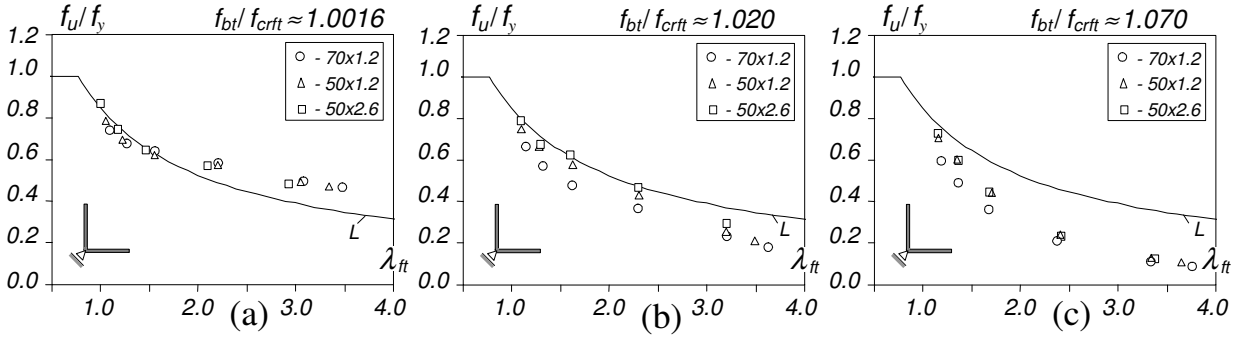

Figure 6: Plots of f_u/f_y against λ_{ft} for f_{bt}/f_{crft} values roughly equal to (a) *1.002*, (b) *1.020* and (c) *1.070*

(ii) To propose a set of curves, defined by "Winter-type" expressions (similar to the current DSM local strength curve – Eq. (1)), to estimate the column flexural-torsional strengths (f_{nft}) as accurately as possible. Such set of curves is of the form

$$f_{nft} = \begin{cases} f_y & \text{if} \quad \lambda_{ft} \le \left(0.5 + \sqrt{0.25 - b}\right)^{\frac{1}{2a}} \\ f_y \left(\frac{f_{crft}}{f_y}\right)^a \left[1 - b\left(\frac{f_{crft}}{f_y}\right)^a\right] & \text{if} \quad \lambda_{ft} > \left(0.5 + \sqrt{0.25 - b}\right)^{\frac{1}{2a}} \end{cases} \quad \text{with} \quad \lambda_{ft} = \sqrt{\frac{f_y}{f_{crft}}} \quad , \qquad (9)$$

and each individual curve corresponds to a different combination of the parameters a and b, through which the column strength length-dependence is captured. Both parameters are expressed in terms of the ratio Δ_f, defined by

$$\Delta_f = \frac{f_{bt} - f_{crft}}{f_{crft}} \times 100 \quad , \qquad (10)$$

and quantifying the weakening effect of major-axis flexure on the column post-critical strength – note that the availability of the analytical expressions given in Eqs. (7) and (8) renders the calculation of Δ_f a very straightforward matter.

(iii) To obtain, through a "trial-and-error curve-fitting procedure" based on the available numerical failure load data (*170* columns continuously restrained against minor-axis flexure – see Fig. 5(a)), expressions providing parameters a and b on the sole basis of Δ_f. Adopting a=*0.4* and b=*0.15* for

$\Delta_f=0$, which amounts to saying that Eqs. (9) and (1) coincide for the shorter columns (f_{br}/f_{crft} very close to *1*)[11], it was possible to reach the following sets of expressions for parameters *a* and *b*:

$$a=\begin{cases} -0.010\,\Delta_f^2+0.240\,\Delta_f+0.400 & if \quad \Delta_f \le 0.4 \\ -0.020\,\Delta_f^2+0.200\,\Delta_f+0.418 & if \quad 0.4>\Delta_f>4.0 \\ 0.002\,\Delta_f+0.889 & if \quad \Delta_f \ge 4.0 \end{cases}, \tag{11}$$

$$b=\begin{cases} -0.220\,\Delta_f^2+0.280\,\Delta_f+0.150 & if \quad \Delta_f \le 1.0 \\ 0.010\,\Delta_f+0.200 & if \quad 1.0<\Delta_f<4.9 \\ 0.249 & if \quad \Delta_f \ge 4.9 \end{cases}. \tag{12}$$

Fig. 7(a) plots f_u/f_y (white dots) and f_{nft}/f_y (grey dots) against λ_{ft}, for all the continuously restrained columns analyzed in this work – also depicted in this figure is the current DSM local strength curve. As for Figs. 7(b_1)-(b_3), they show the flexural-torsional strength curves obtained from Eq. (9) for $\Delta_f=0.16;1.80;7.20$ – also included are the numerical failure loads that are supposed to be predicted by these three strength curves. The observation of these results prompts the following remarks:

(i) Fig. 7(a) shows that the f_{nft} strength curves (grey dots) are able to capture the "vertical dispersion" of the numerical ultimate strengths (white dots).

(ii) Indeed, the three curves shown in Fig. 7(b) follow the f_{nft} trends reasonably well, in the sense that they provide more or less accurate underestimations of the numerical failure loads.

(iii) For the shorter columns ($\Delta_f=0.16$), the strength curve provides rather accurate predictions for $\lambda_{ft}<1.5$ and considerable underestimations for higher slenderness values.

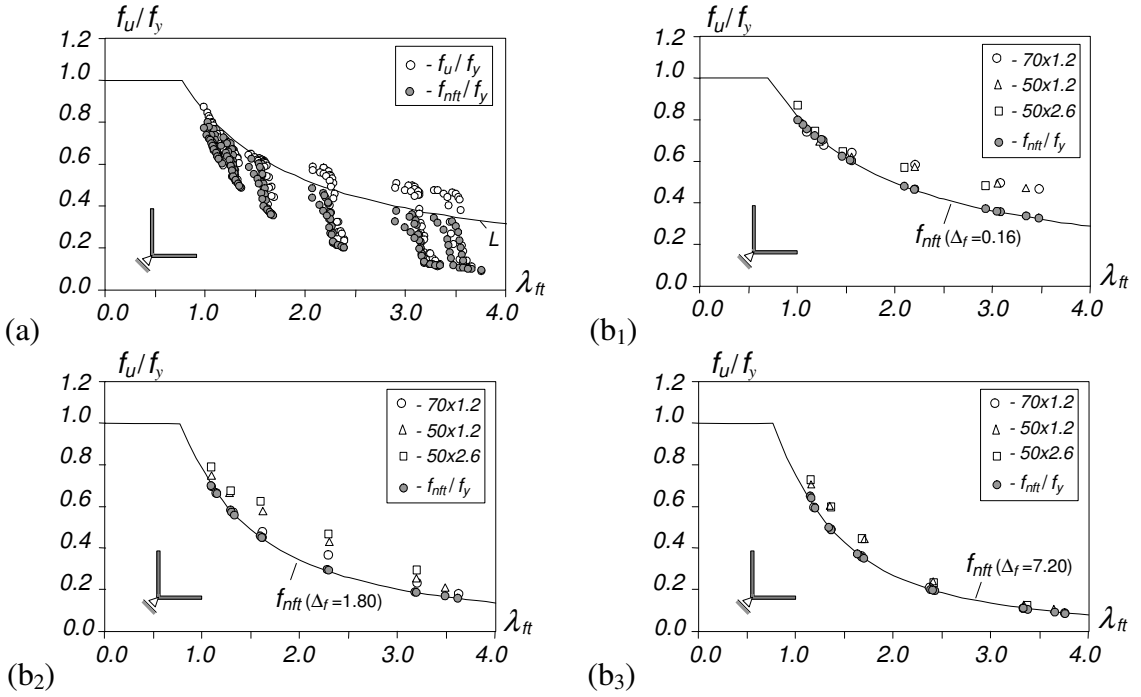

Figure 7: (a) Plots of f_u/f_y and f_{nft}/f_y, against λ_{ft}, for all restrained columns analyzed in this work, and (b) proposed f_{nft} strength curves for (b_1) $\Delta_f=0.16$, (b_2) *1.80* and (b_3) *7.20* and the numerical failure loads predicted by each of them

[11] It was found that the DSM local strength curve predicts reasonably well the numerical ultimate strengths of the shorter columns.

(iv) For the longer columns (Δ_f=*7.20*), the strength curve provides reasonable predictions for the whole slenderness range.

(v) The most conservative predictions concern the intermediate columns (Δ_f=*1.80*).

5.2 DSM-Based Design Approach for Fixed-Ended Columns

The proposed DSM-based approach to design fixed-ended equal-leg angle columns, which generally fail in flexural-torsional/flexural interactive modes, consists of combining Eq. (9) with the current DSM global strength curve, given in Eq. (2). Following the strategy adopted in the current DSM design against local-global interactive failures, f_y is replaced by f_{ne} in Eq. (9), leading to the f_{nfte}^F ultimate strength estimates

$$f_{nfte}^F = \begin{cases} f_{ne} & \text{if} \quad \lambda_{fte} \le \left(0.5+\sqrt{0.25-b}\right)^{\frac{1}{2a}} \\ f_{ne}\left(\frac{f_{crft}}{f_{ne}}\right)^a \left[1-b\left(\frac{f_{crft}}{f_{ne}}\right)^a\right] & \text{if} \quad \lambda_{fte} > \left(0.5+\sqrt{0.25-b}\right)^{\frac{1}{2a}} \end{cases} \quad \text{with} \quad \lambda_{fte} = \sqrt{\frac{f_{ne}}{f_{crft}}} \quad . \qquad (13)$$

5.3 DSM-Based Design Approach for Pin-Ended Columns

As shown earlier, the strength differences between P and F columns stem from the effective centroid shift effects. Thus, a rational procedure must be found before it is possible to propose a DSM-based approach to design pin-ended equal-leg angle columns. The procedure adopted follows Rasmussen's (2006) idea: incorporate the effective centroid shift through a multiplicative parameter β depending also on the column slenderness – then, the column ultimate strength is obtained by multiplying the F column ultimate strength prediction (f_{nfte}^F) by the parameter β, *i.e.*,

$$f_{nfte}^P = \beta \cdot f_{nfte}^F \quad . \qquad (14)$$

The procedure adopted to search for an expression providing the parameter β is based on an "elastic reduction factor" concept that accounts for the fact that both the post-buckling strength and effective centroid shift effects vary substantially with the column length – naturally, attention is restricted to short-to-intermediate lengths, *i.e.*, those corresponding to the P column $P_{cr}(L)$ curve plateau. This procedure involves the following steps:

(i) Perform elastic post-buckling analyses of geometrically identical F and P columns (sharing the same f_{bt}/f_{crft} ratio and critical-mode initial geometrical imperfections with amplitude *L/1000*) and record the evolution, as the applied load increases, of the maximum longitudinal normal stresses (f_{max}), occurring at the mid-span cross-section. For illustrative purposes, Fig. 8(a) displays the P vs. f_{max} curves concerning F and P columns associated with Δ_f=*0.16* (f_{bt}/f_{crft}=*1.0016*).

(ii) Assume that, for a given f_{max} value, the difference between the F and P column applied loads (P_F and P_P) stems exclusively from the effective centroid shift effects – then, the P_P/P_F ratio provides a good approximation for the parameter β (*i.e.*, it is assumed that $\beta \approx P_P/P_F$)[12].

(iii) Relate f_{max} with the column slenderness by means of $\lambda_{ft}=(f_{max}/f_{crft})^{0.5}$, which amounts to assuming that β is the strength reduction due to the effective centroid shift effects at the "elastic limit state". Then, it becomes possible to develop $\beta(\lambda_{ft})$ curves, one for each Δ_f value, which will be incorporated

[12] When the P column elastic non-linear equilibrium path exhibits a limit point (this happens in a few cases – see Fig. 2(b)), it is assumed that the corresponding P vs. f_{max} curve (see Fig 8(a)) becomes a horizontal straight line beyond that limit point – *i.e.*, the value of P_P remains constant.

into Eq. (15). For illustrative purposes, Fig. 8(b) displays the $\beta(\lambda_{ft})$ curves concerning the columns associated with Δ_f=*0.16*;*0.84*;*2.41*. The differences between these curves clearly show that the relation $\beta(\lambda_{ft})$ varies with the angle column length – β decreases substantially as the length increases. Fig. 8(b) also includes the $\beta(\lambda_{ft})$ curve proposed by Rasmussen (2006) and given in Eq. (4c)[13] – note that this curve is well above its upper $\beta(\lambda_{ft})$ counterpart.

(iv) By means of a second "trial-and-error curve-fitting procedure", look for "Winter-type" expressions relating parameter β with the column flexural-torsional slenderness λ_{ft}, of the form

$$\beta = \frac{0.68}{(\lambda_{ft} - c)^d} \leq 1 \quad , \tag{15}$$

where the dependency of β on the column length is felt through parameters c and d, which are expressed as functions of the ratio Δ_f. On the basis of the numerical results obtained and adopting c=*1.0* and d=*0.25* for Δ_f=*0*, which amounts to saying that Eqs. (15) and (4c) coincide for the shorter columns (f_{bt}/f_{crft} very close to *1*)[14], the following expressions for parameters c and d are proposed:

$$c = \begin{cases} -39.0\ \Delta_f + 1.000 & \text{if} \quad \Delta_f \leq 0.01 \\ 0.610 & \text{if} \quad 0.01 < \Delta_f < 0.15 \\ -2.600\ \Delta_f + 1.000 & \text{if} \quad 0.15 < \Delta_f < 0.20 \\ -0.144\ \Delta_f + 0.509 & \text{if} \quad 0.20 < \Delta_f < 3.5 \\ 0.005 & \text{if} \quad \Delta_f \geq 3.5 \end{cases} \quad , \tag{16}$$

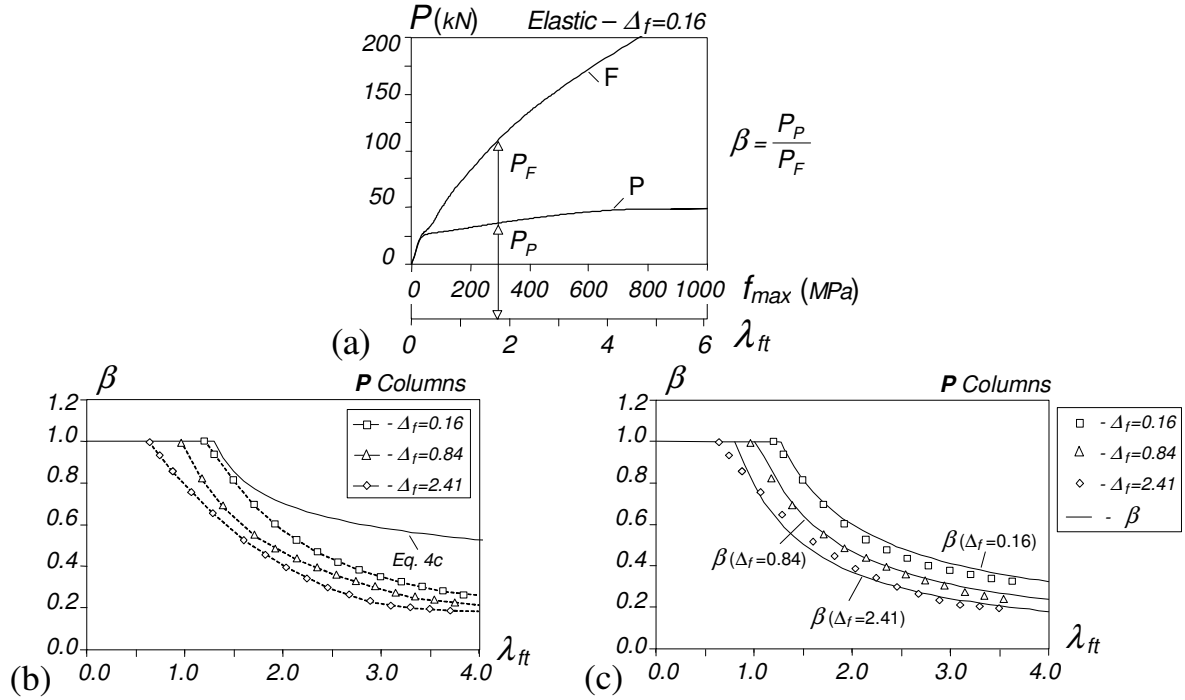

Figure 8: (a) P vs. f_{max} curves concerning F and P columns (Δ_f=*0.16*), (b) numerically obtained $\beta(\lambda_{ft})$ curves associated with Δ_f=*0.16*;*0.84*;*2.41*, and (c) proposed $\beta(\lambda_{ft})$ expressions for Δ_f=*0.0*;*0.16*;*0.84*;*2.41*, compared with the numerical values

[13] Rasmussen based his curve on local buckling concepts and, therefore, he viewed it as a $\beta(\lambda_l)$ curve.

[14] It was found that the β parameter proposed by Rasmussen (2006) leads to reasonable predictions of the numerical ultimate strengths of the shorter P columns.

$$d = \begin{cases} 42.0\ \Delta_f + 0.250 & if \quad \Delta_f \le 0.01 \\ 0.670 & if \quad 0.01 < \Delta_f < 0.15 \\ 2.800\ \Delta_f + 0.250 & if \quad 0.15 < \Delta_f < 0.20 \\ 0.077\ \Delta_f + 0.795 & if \quad 0.20 < \Delta_f < 3.5 \\ 0.001\ \Delta_f + 1.064 & if \quad \Delta_f \ge 3.5 \end{cases} \quad . \tag{17}$$

Fig. 8(c) displays (i) the β *vs.* λ_{ft} curves provided by Eqs. (15)-(17) for columns exhibiting Δ_f=*0.0*;*0.16*; *0.84*;*2.41*, and (ii) the corresponding numerical β values (for $\Delta_f \neq 0.0$). It is observed that the curves follow reasonably well the "numerical result trends", even if there are some visible differences − the most relevant ones concern the very slender shorter columns (Δ_f=*0.16*). Finally, note that, since β is used to lower the interactive strength f_{nfte}^{F}, it is just logical to express Eq. (15) in terms of the "interactive slenderness" λ_{fte}, instead of its flexural-torsional counterpart λ_{ft}.

5.4 Summary of the Proposed DSM Design Approaches

The proposed DSM-based approaches for the design of fixed-ended and pin-ended equal-leg angle columns can be cast in a unified form, by means of the expressions[15]

$$f_{nfte} = \begin{cases} \beta \cdot f_{ne} & if \quad \lambda_{fte} \le \left(0.5 + \sqrt{0.25 - b}\right)^{\frac{1}{2a}} \\ \beta \cdot f_{ne} \left(\frac{f_{crft}}{f_{ne}}\right)^{a} \left[1 - b \left(\frac{f_{crft}}{f_{ne}}\right)^{a}\right] & if \quad \lambda_{fte} > \left(0.5 + \sqrt{0.25 - b}\right)^{\frac{1}{2a}} \end{cases} \quad \text{with } \lambda_{fte} = \sqrt{\frac{f_{ne}}{f_{crft}}} \quad , \tag{18}$$

$$a = \begin{cases} -0.010\ \Delta_f^2 + 0.240\ \Delta_f + 0.400 & if \quad \Delta_f \le 0.4 \\ -0.020\ \Delta_f^2 + 0.200\ \Delta_f + 0.418 & if \quad 0.4 > \Delta_f > 4.0 \\ 0.002\ \Delta_f + 0.889 & if \quad \Delta_f \ge 4.0 \end{cases} \quad , \tag{19}$$

$$b = \begin{cases} -0.220\ \Delta_f^2 + 0.280\ \Delta_f + 0.150 & if \quad \Delta_f \le 1.0 \\ 0.010\ \Delta_f + 0.200 & if \quad 1.0 < \Delta_f < 4.9 \\ 0.249 & if \quad \Delta_f \ge 4.9 \end{cases} \quad , \tag{20}$$

$$\beta = \begin{cases} 1 & for\ F\ columns \\ \dfrac{0.68}{(\lambda_{fte} - c)^{d}} \le 1 & for\ P\ columns \end{cases} \quad , \tag{21}$$

$$c = \begin{cases} -39.0\ \Delta_f + 1.000 & if \quad \Delta_f \le 0.01 \\ 0.610 & if \quad 0.01 < \Delta_f < 0.15 \\ -2.600\ \Delta_f + 1.000 & if \quad 0.15 < \Delta_f < 0.20 \\ -0.144\ \Delta_f + 0.509 & if \quad 0.20 < \Delta_f < 3.5 \\ 0.005 & if \quad \Delta_f \ge 3.5 \end{cases} \quad , \tag{22}$$

[15] It is worth recalling that (i) $\Delta_f = [(f_{bt} - f_{crft}) / f_{crft}] \times 100$ and (ii) f_{bt} and f_{crft} can be straightforwadly calculated through Eqs. (7)-(8).

$$d = \begin{cases} 42.0\ \Delta_f + 0.250 & if \quad \Delta_f \le 0.01 \\ 0.670 & if \quad 0.01 < \Delta_f < 0.15 \\ 2.800\ \Delta_f + 0.250 & if \quad 0.15 < \Delta_f < 0.20 \\ 0.077\ \Delta_f + 0.795 & if \quad 0.20 < \Delta_f < 3.5 \\ 0.001\ \Delta_f + 1.064 & if \quad \Delta_f \ge 3.5 \end{cases} \quad . \tag{23}$$

5.5 Assessment of the Proposed DSM Design Approaches

Attention is now turned to assessing the performance of the proposed two DSM-based design procedures (f_{nfte} estimates), namely the DSM-F and DSM-P approaches. Their predictions (f_{nfte}) for the whole set of experimental and numerical column ultimate strengths gathered are given in the tables included in Annexes B-E, together with the corresponding failure-to-predicted strength ratios f_u/f_{nfte} – while Annexes B and C concern the experimental results, Annexes D and E deal with the numerical ones. Figs. 9(a)-(b) plot the f_u/f_{nfte} (failure-to-predicted) ratios against λ_{fte} for the whole set of experimental and numerical F and P column ultimate strengths – the associated averages, standard deviations and maximum/minimum values are given in Table 2. The observation of these results prompts the following remarks:

(i) The DSM-F procedure leads to quite accurate predictions of the experimental and numerical ultimate strengths – the f_u/f_{nfte} averages and standard deviations are (i_1) *1.00/0.11* (experimental), (i_2) *1.02/0.11* (numerical results) and (i_3) *1.02/0.11* (experimental + numerical).

(ii) The DSM-P procedure also leads to very good estimates of the experimental and numerical ultimate strengths – the f_u/f_{nfte} averages and standard deviations are now (ii_1) *1.05/0.21* (experimental), (ii_2) *1.06/0.07* (numerical results) and (ii_3) *1.06/0.10* (experimental + numerical).

(iii) The quality of the above performance indicators (iii_1) provides solid evidence concerning the adequacy of the reasoning behind the development of the flexural-torsional strength (F and P columns) and β vs. λ_{fte} (P columns) curves, and (iii_2) also indicates that the outputs of these curves reflect quite accurately the underlying structural concepts.

(iv) The comparison between the values presented in Tables 1 and 2[16] makes it possible to conclude that the proposed design approach has performance indicators that are equal or slightly better than those concerning the proposals developed by Young (2004) (F columns), Rasmussen (2006) (P columns) and Silvestre *et. al.* (2013) (F and P columns). However, it has the very important advantage of being clearly more rational – indeed the new proposals reflect quite closely the angle column structural behavior and also retain the current DSM global strength curve. Moreover, the analytical expressions given in Eqs. (7) and (8) ensure their straightforward and easy application.

(v) Finally, just two words to mention that all available P column test results (failure loads) correspond to a fairly narrow and relatively low slenderness range, thus showing the need to obtain experimental data concerning more slender P columns (to ensure proper validation for design approaches). Moreover, unlike their numerical counterparts, the P column experimental failure loads exhibit a quite large scatter, which is primarily due to a very high sensitivity to the initial minor-axis flexural imperfection sign (Mesacasa Jr. *et al.* 2013)[17] – the most detrimental sign, *i.e.*, that reinforcing the effective centroid shift effects, was always considered when determining the numerical failure loads.

[16] It should be pointed out that Table 2 is based on a considerably larger numerical F and P colum failure load data bank.

[17] For instance, look at the identical test trios reported by Wilhoite *et al.* (1984): while (i) the three shorter columns had very similar ultimate strengths, (ii) the intermediate columns showed some scatter (higher and lower ultimate strengths *11.5%* apart) and (iii) the longer columns exhibited an even higher scatter (*22.5%* difference).

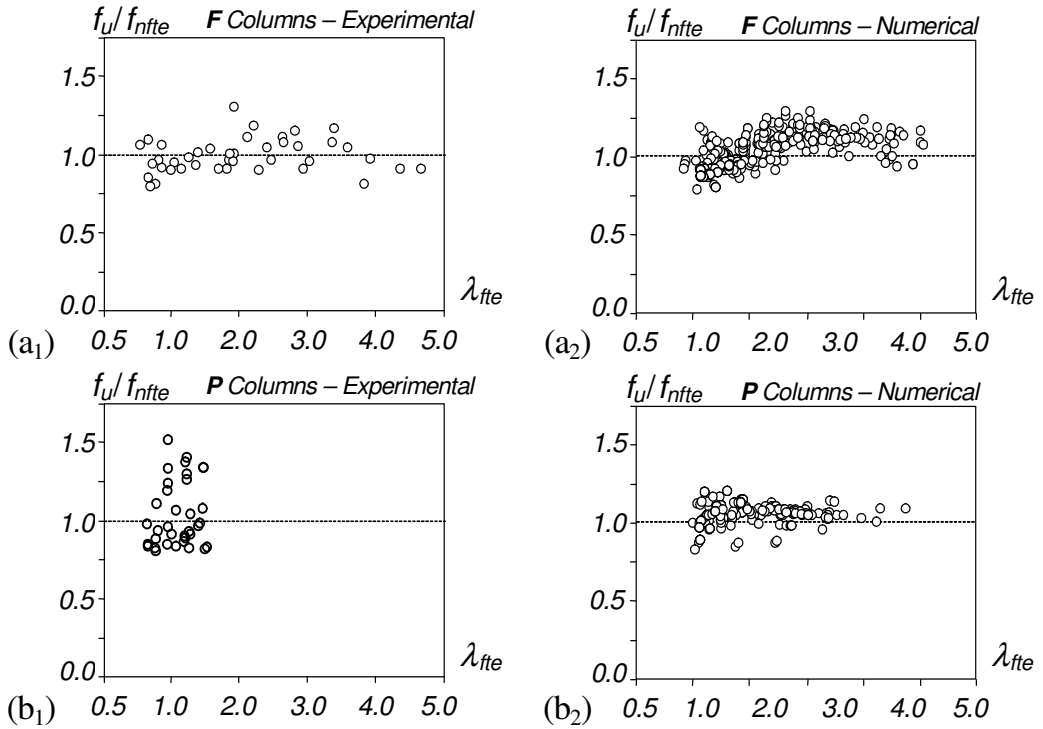

Figure 9: Plots of f_u/f_{nfte}, against λ_{fte}, for the (a) F and (b) P columns: $(_1)$ experimental and $(_2)$ numerical results

Table 2: Means, standard deviations and maximum/minimum values of the failure-to-predicted strength ratios provided by the proposed DSM design approaches for the F and P column experimental, numerical and "experimental + numerical" results

	DSM-F approach			DSM-P approach		
	Exp.	Num	Exp+Num	Exp	Num	Exp+Num
Mean	1.00	1.02	1.02	1.05	1.06	1.06
Sd. Dev.	0.11	0.11	0.11	0.21	0.07	0.10
Max	1.31	1.29	1.31	1.53	1.20	1.53
Min	0.80	0.79	0.79	0.82	0.83	0.82

Load and Resistance Factor Design (*LRFD*)

The evaluation of the LRFD (Load and Resistance Factor Design) resistance factor ϕ associated with the proposed DSM-based approaches is addressed next. According to the North American cold-formed steel specification (AISI 2012), ϕ can be calculated using the formula given in section F.1.1 of chapter F,

$$\phi = C_\phi (M_m F_m P_m)\, e^{-\beta_0 \sqrt{V_M^2 + V_F^2 + C_P V_P^2 + V_Q^2}} \qquad \text{with} \quad C_P = \left(1 + \frac{1}{n}\right)\frac{m}{m-2} \qquad , \quad (22)$$

where (i) C_ϕ is a calibration coefficient (C_ϕ=*1.52* for LRFD), (ii) M_m=*1.0* and F_m=*1.00* are the mean values of the material and fabrication factor, respectively, (iii) β_0 is the target reliability index (β_0=*2.5* for structural members in LRFD), (iv) V_M=*0.10*, V_F=*0.05* and V_Q=*0.21* are the coefficients of variation of the material factor, fabrication factor and load effect, respectively, and (v) C_P is a correction factor that

depends on the numbers of tests (n) and degrees of freedom ($m=n-1$). In order to evaluate ϕ for each proposed DSM procedure (DSM-F and DSM-P), it is necessary to calculate P_m and V_P, which are the mean and standard deviation of the "exact"-to-predicted strength ratios f_u/f_{nfte} – the "exact" f_u values are either experimental, numerical or experimental and numerical.

Tables 3 and 4 show the n, C_P, P_m, V_P and ϕ values obtained for the column ultimate strength predictions provided by the DSM-F and DSM-P procedures applied to the experimental, numerical and total failure load data – also indicated are the values (i) reported by Silvestre *et. al.* (2013) and (ii) determined with the design proposals of Young (2004) and Rasmussen (2006). It is observed that:

(i) When the whole (experimental and numerical) failure load data are considered, the resistance factor values associated with each proposed DSM-based procedure are (i_1) $\phi=0.86$ (F columns) and $\phi=0.78$ (P columns), for the experimental data, (i_2) $\phi=0.89$ (F columns) and $\phi=0.95$ (P columns), for the numerical data, and (i_3) $\phi=0.89$ (F columns) and $\phi=0.92$ (P columns), for the experimental and numerical data. These values are almost perfectly in line with the recommendations of the North American specification for cold-formed steel compression members ($\phi=0.85$ –AISI 2012), which are currently not applicable to angles (Ganesan & Moen 2012).

(ii) The ϕ values obtained with the whole failure load data bank are either very similar or slightly above those achieved by Silvestre *et al.* (2013). Moreover they are slightly below and above those provided by the proposals of Young (2004), for F columns, and Rasmussen (2006), for P columns – recall that these authors only employed their proposals to estimate experimental column failure loads (all the predictions concerning numerical ultimate strengths were carried out in this work).

Table 3: LRFD resistance factors ϕ calculated according to AISI (2012) – DSM-F procedure and proposals from Silvestre *et al.* (2013) and Young (2004)

	DSM-F approach			Silvestre *et al.* (2013)			Young (2004)		
	Exp	Num	Exp+Num	Exp	Num	Exp+Num	Exp	Num	Exp+Num
n	41	337	378	41	89	130	41	89	130
C_P	1.078	1.009	1.008	1.078	1.035	1.024	1.078	1.035	1.024
P_m	0.998	1.024	1.022	0.980	1.023	1.010	1.135	1.142	1.139
V_P	0.109	0.112	0.111	0.145	0.105	0.120	0.182	0.157	0.165
ϕ	0.86	0.89	0.89	0.81	0.89	0.87	0.89	0.93	0.92

Table 4: LRFD resistance factors ϕ calculated according to AISI (2012) – DSM-P procedure and proposals from Silvestre *et al.* (2013) and Rasmussen (2006)

	DSM-P approach			Silvestre *et al.* (2013)			Rasmussen (2006)		
	Exp	Num	Exp+Num	Exp	Num	Exp+Num	Exp	Num	Exp+Num
n	35	197	232	35	28	63	35	28	63
C_P	1.093	1.015	1.013	1.093	1.119	1.050	1.093	1.119	1.050
P_m	1.045	1.057	1.055	1.136	1.103	1.110	1.089	1.020	1.058
V_P	0.211	0.071	0.104	0.246	0.111	0.196	0.243	0.145	0.208
ϕ	0.78	0.95	0.92	0.78	0.95	0.85	0.76	0.84	0.80

(iii) There is quite solid evidence that $\phi=0.85$ can be also recommended for cold-formed steel angle compression members designed by means of the DSM-F and DSM-P procedures. Although this feature was already shared by the proposals developed by Young (2004) (F columns) and Silvestre *et al.* (2013) (F and P columns)[18], the structural clarity and rationality of the approaches proposed in this work is definitely a significant advantage.

6. Conclusion

This work dealt with the development and assessment of novel procedures for the design of fixed-ended (F) and pin-ended (P) equal-leg angle columns with short-to-intermediate lengths, *i.e.*, those buckling in flexural-torsional modes. Initially, numerical results concerning the buckling and post-buckling behavior of the above angle columns were briefly presented, (i) highlighting the main differences between the F and P column responses, and (ii) evidencing the need for specific design procedures. Then, the paper gathered a large column ultimate strength data bank that included (i) experimental values, collected from the available literature and concerning *41* fixed-ended and *35* pin-ended columns, and (ii) numerical values, obtained from ABAQUS shell finite element analyses and involving *372* fixed-ended and *197* pin-ended (cylindrical supports) columns with various cross-section dimensions, lengths and yield stresses.

Next, after reviewing the most efficient available methods to estimate failure loads of short-to-intermediate angle columns, the paper presented the development of novel rational DSM-based procedures to design such members. The mechanical reasoning behind these procedures is based on the fact that (i) both the F and P columns fail in interactive modes, combining (major-axis) flexural-torsional and (minor-axis) flexural deformations, and that (ii) the above interaction is much stronger in the P columns, due to the presence of effective centroid shift effects. In order to incorporate these behavioral features in the DSM design approach, it was necessary to find efficient/accurate ways to quantify (i) the F and P column flexural-torsional strength and (ii) the P columns effective centroid shift effects. These two tasks were performed numerically and led to the development of (i) genuine flexural-torsional strength curves, intended to play the role of the local strength curve in the traditional column design against local-global interactive failure, and (ii) curves providing a parameter able to capture the ultimate strength erosion stemming from the effective centroid shifts. Since the two sets of curves were found to be quite strongly length-dependent, their definition included the percentage ratio between the column pure torsional and flexural-torsional buckling loads, which is able to capture the above length-dependency, essentially linked to the participation of the minor-axis flexural deformations in the column failure modes – analytical expressions were developed to calculate the angle column torsional and flexural-torsional buckling loads, thus making the application of the proposed DSM-based procedures straightforward and easy.

Finally, the paper closed with the assessment of the ultimate strength predictions provided by the proposed DSM design approach, by comparing them with the assembled experimental and numerical (ABAQUS SFEA) failure load data bank. Both the quality and reliability of these predictions were found to be very good and, in particular, it was shown that the LRFD resistance factor $\phi=0.85$, currently prescribed in AISI (2012) for member design, can also be safely adopted for the angle columns ultimate strength predictions provided by the proposed DSM design approaches (currently, angle columns are explicitly excluded from the domain of application of these specifications). Moreover, these novel DSM design approaches exhibit performance indicators that compare favorably with those concerning the proposals of Young (2004) (F columns), Rasmussen (2006) (P columns) and Silvestre *et. al.* (2013) (F and P

[18] The proposal of Rasmussen (2006) (P columns) exhibits slightly lower ϕ values.

columns) – moreover, it has the very important advantage of being clearly more rational, in the sense that it reflects closely the angle column structural behavior and retains the current DSM global strength curve.

It still worth mentioning that the authors are currently working on extending the DSM design approaches proposed in this work to cover (i) pin-ended angle columns with spherically-hinged supports and (ii) hot-rolled steel angle columns, which normally exhibit considerably less slender legs (lower width-to-thickness ratios) and whose structural response may be visibly influenced by residual stress effects.

References

AISI (American Iron and Steel Institute) (2012). *North American Specification for the Design of Cold-Formed Steel Structural Members* (NAS), Washington DC.

AS/NZS (Standards of Australia and Standards of New Zealand) (2005). *Cold-Formed Steel Structures*, Sydney-Wellington.

Bebiano R, Silvestre N, Camotim D (2008a). "*GBTUL 1.0β – Code for Buckling and Vibration Analysis of Thin-Walled Members*", freely available at *http://www.civil.ist.utl.pt/gbt*.

Bebiano R, Silvestre N, Camotim D (2008b). "GBTUL – a code for the buckling analysis of cold-formed steel members", *Proceedings of 19th International Specialty Conference on Recent Research and Developments in Cold-Formed Steel Design and Construction* (St. Louis, 14-15/10), R. LaBoube, W.-W. Yu (eds.), 61-79.

Chodraui GMB, Shifferaw Y, Malite M, Schafer BW (2006). "Cold-formed steel angles under axial compression", *Proceedings of 18th International Specialty Conference on Cold-Formed Steel Structures* (Orlando, 26-27/10), R. LaBoube, W.W. Yu (eds.), 285-300.

Dinis PB, Camotim D (2011). "Buckling, post-buckling and strength of equal-leg angle and cruciform columns: similarities and differences", *Proceedings of 6th European Conference on Steel and Composite Structures* (EUROSTEEL 2011 – Budapest, 31/8-2/9), L. Dunai, M. Iványi, K. Jármai, N. Kovács, L.G. Vigh (eds.), ECCS (Brussels), 105-110 (vol. A).

Dinis PB, Camotim D, Silvestre N (2010a). "Post-buckling behaviour and strength of angle columns", *Proceedings of International Colloquium on Stability and Ductility of Steel Structures* (SDSS'10 Rio – Rio de Janeiro, 8-10/9), E. Batista, P. Vellasco, L. Lima (eds.), 1141-1150.

Dinis PB, Camotim D, Silvestre N (2010b). "On the local and global buckling behaviour of angle, T-section and cruciform thin-walled columns and beams", *Thin-Walled Structures*, **48**(10-11), 786-797.

Dinis PB, Camotim D, Silvestre N (2011). "On the design of steel angle columns", *Proceedings of 6th International Conference on Thin-Walled Structures* (ICTWS 2011 – Timisoara, 5-7/9), D. Dubina, V. Ungureanu (eds.), 271-279.

Dinis PB, Camotim D, Silvestre N (2012). "On the mechanics of angle column instability", *Thin-Walled Structures*, **52**(March), 80-89.

Dinis PB, Camotim D, Landesmann A (2013). "Towards a more rational DSM design approach for angle columns", *USB Key Drive Proceedings of the SSRC Annual Stability Conference* (St. Louis, 16-20/4), 2013.

Ellobody E, Young B (2005). "Behavior of cold-formed steel plain angle columns", *Journal of Structural Engineering* (ASCE), **131**(3), 469-478.

Ganesan K, Moen CD (2012). "LRFD resistance factor for cold-formed steel compression members", *Journal of Constructional Steel Research*, **72**(May), 261-266.

Kitipornchai S, Chan SL (1987). "Nonlinear finite-element analysis of angle and tee beam-columns", *Journal of Structural Engineering* (ASCE), **113**(4), 721-739.

Kitipornchai S, Albermani FGA, Chan SL (1990). "Elastoplastic finite-element models for angle steel frames", *Journal of Structural Engineering* (ASCE), **116**(10), 2567-2581.

Maia WF, Neto JM, Malite M (2008). "Stability of cold-formed steel simple and lipped angles under compression", *Proceedings of 19th International Specialty Conference on Cold-Formed Steel Structures* (St. Louis, 26-27/10), R. LaBoube, W.W. Yu (eds.), 111-125.

Mesacasa Jr. EC (2012). *Structural Behavior and Design of Cold-Formed Steel Angle Columns*, M.A.Sc. Thesis in Structural Engineering, School of Engineering at São Carlos, University of S. Paulo, Brazil. (Portuguese)

Mesacasa Jr. E, Dinis PB, Camotim D, Malite M (2013). "Mode interaction and imperfection-sensitivity in thin-walled equal-leg angle columns", *Thin-Walled Structures*, in press.

Popovic D, Hancock GJ, Rasmussen KJR (1999). "Axial compression tests of cold-formed angles", *Journal of Structural Engineering* (ASCE), **125**(5), 515-523.

Rasmussen KJR (2005). "Design of angle columns with locally unstable legs", *Journal of Structural Engineering* (ASCE), **131**(10), 1553-1560.

Rasmussen KJR (2006). "Design of slender angle section beam-columns by the direct strength method", *Journal of Structural Engineering* (ASCE), **132**(2), 204-211.

Schafer BW (2008). "Review: the direct strength method of cold-formed steel member design", *Journal of Constructional Steel Research*, **64**(7-8), 766-778.

Shi G, Liu Z, Chung KF (2009). "Numerical study on the local buckling of 420 MPa steel equal angle columns under axial compression", *Proceedings of 6th International Conference on Advances in Steel Structures* (ICASS'09 – Hong Kong, 16-18/12), S.L. Chan (ed.), 387-394 (vol. I).

Shifferaw Y, Schafer BW (2011). "Behavior and design of cold-formed steel lipped and plain angles", *USB Proceedings of SSRC Annual Stability Conference* (Pittsburgh, 10-14/5).

Simulia Inc. (2008). *Abaqus Standard* (vrs. 6.7-5).

Silvestre N, Dinis PB, Camotim D (2013). "Developments on the Design of Cold-Formed Steel Angles", *Journal of Structural Engineering* (ASCE), **139**(5), 680-694.

Stowell EZ (1951). *Compressive Strength of Flanges*, National Advisory Committee for Aeronautics (NACA), Report Nº 1029.

Wilhoite GM, Zandonini R, Zavelani A (1984). "Behaviour and strength of angles in compression: an experimental investigation", *Proceedings of ASCE Annual Convention and Structures Congress* (San Francisco, 1-3/10).

Young B (2004). "Tests and design of fixed-ended cold-formed steel plain angle columns", *Journal of Structural Engineering* (ASCE), **130**(12), 1931-1940.

Young B, Rasmussen KJR (1999). "Shift of effective centroid in channel columns", *Journal of Structural Engineering* (ASCE), **125**(5), 524-531.

ANNEX A: TORSIONAL AND FLEXURAL-TORSIONAL BUCKLING LOAD FORMULAE

This annex presents the derivation of (i) analytical expressions to calculate the torsional (P_{bt}) and flexural-torsional (P_{crft} – critical) buckling loads in fixed-ended equal-leg (width b, thickness t, length L) steel (E, $G=E/2(1+\nu)$) angle columns – see Figure A.1, where y and z denote axes that are parallel to the cross-section centroidal principal axes and pass through its shear center (C).

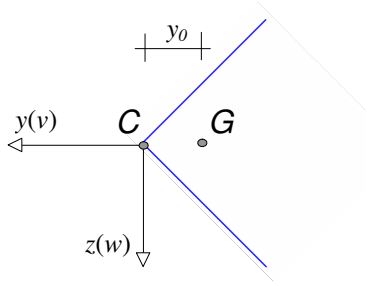

Figure A.1: Equal-leg angle column cross-section geometry

The quadratic term of the column total potential energy (V) reads

$$V_2 \equiv V = U + V_e \quad , \tag{A.1}$$

where U is the columns strain energy and V_e is the potential of the applied axial load, given by

$$U = \frac{1}{2}\int_0^L \left[EI_1 w_{,xx}^2 + GJ\phi_{,x}^2 + EI_w\phi_{,x}^2\right]dx \quad , \tag{A.2}$$

$$V_e = -P\Delta = -\frac{1}{2}\int_0^L \left[w_{,x}^2 + r_0^2\,\phi_{,x}^2 + 2\,y_0\,w_{,x}\,\phi_{,x}\right]dx \quad . \tag{A.3}$$

In these expressions, (i) EI_y is the major-axis bending stiffness, (ii) GJ is the Saint-Venant (uniform) torsion stiffness, (iii) EI_w is the warping (non-uniform torsion) stiffness, (iv) Δ is the column axial shortening, (v) ϕ is the torsional rotation and (vi) r_0 is the cross-section polar radius of gyration with respect to its shear center C, defined by

$$r_0^2\,A = \int_A y^2 + z^2\,dA \quad . \tag{A.4}$$

The two Euler-Lagrange equations ensuring $\delta V = 0$ (adjacent equilibrium condition) are

$$EI_y\,w_{,xxxx} + P\left(w_{,xx} + y_0\,\phi_{,xx}\right) = 0 \quad , \tag{A.5}$$

$$EI_w\,\phi_{,xxxx} - GJ\phi_{,xx} + P\left(r_0^2\,\phi_{,xx} + w_0\,\phi_{,xx}\right) = 0 \quad , \tag{A.6}$$

and their joint solution, together with the appropriate boundary conditions, provides the column buckling loads (eigenvalues) and buckling mode shapes (eigenfunctions). In the case of fixed-ended columns, adopting the Galerkin method and assuming the column buckling mode is of the form

$$w = C_1 \sin\frac{\pi x}{L}\,\sin\frac{\pi x}{L} \quad , \tag{A.7}$$

$$\phi = C_2 \sin\frac{\pi x}{L} \sin\frac{\pi x}{L} \quad , \tag{A.8}$$

one is led to the eigenvalue problem defined by the linear algebraic equilibrium equation system

$$\begin{bmatrix} (P_{bf} - P) & -P\,y_0 \\ -P\,y_0 & r_0^2 (P_{bt} - P) \end{bmatrix} \begin{Bmatrix} C_1 \\ C_2 \end{Bmatrix} = \begin{Bmatrix} 0 \\ 0 \end{Bmatrix} \quad , \tag{A.9}$$

where

$$P_{bf} = \frac{\pi^2 E I_y}{(L/2)^2} \quad , \tag{A.10}$$

$$P_{bt} = \frac{1}{r_0^2}\left[GJ + \frac{\pi^2 E I_w}{(L/2)^2} \right] \tag{A.11}$$

are the column pure flexural and torsional critical buckling loads. The solution of the corresponding characteristic equation provides the column flexural-torsional buckling load, given by the expression

$$P_{crft} = \frac{r_0^2 (P_{bf} + P_{bt}) - \sqrt{r_0^4 (P_{bf} + P_{bt})^2 - 4\left(r_0^2 - y_0^2\right) P_{bf}\, P_{bt}}}{2\left(r_0^2 - y_0^2\right)} \quad . \tag{A.12}$$

In the particular case of equal-leg angles with leg width b and wall thickness t, the quantities appearing in the previous expressions read[19]

$$I_y = \frac{b^2 t}{3} \qquad J = \frac{2 b t^3}{3} \qquad I_w = \frac{b^3 t^3}{18} \quad , \tag{A.13}$$

$$r_0^2 = \frac{1}{A}\int_A y^2 + z^2\, dA = \frac{b^2}{3} \qquad y_0 = -\frac{b}{2\sqrt{2}} \qquad 2\left(r_0^2 - y_0^2\right) = \frac{5 b^2}{12} \quad , \tag{A.14}$$

which lead to the following expressions for P_{bf}, P_{bt}, P_{crft} (critical buckling load) and the corresponding stress values:

$$P_{bf} = \frac{\pi^2 E\, b^3 t}{3\,(L/2)^2} \qquad f_{bf} = \frac{\pi^2 E\, b^2}{6\,(L/2)^2} \quad , \tag{A.15}$$

$$P_{bt} = G\frac{2\,t^3}{b} + \pi^2 \frac{E\, b\, t^3}{6(L/2)^2} \qquad f_{bt} = G\frac{t^2}{b^2} + \pi^2 \frac{E\, t^2}{12(L/2)^2} \quad , \tag{A.16}$$

$$P_{crft} = \frac{4}{5}\left(P_{bt} + P_{bf} - \sqrt{(P_{bt} + P_{bf})^2 - 2.5\, P_{bt}\, P_{bf}} \right) \quad f_{crft} = \frac{4}{5}\left(f_{bt} + f_{bf} - \sqrt{(f_{bt} + f_{bf})^2 - 2.5\, f_{bt}\, f_{bf}} \right) . \tag{A.17}$$

[19] Note that I_w stems exclusively from secondary warping (the primary warping contribution is obviously null).

ANNEX B: FIXED-ENDED COLUMN EXPERIMENTAL DATA

Table B: Fixed-ended column experimental ultimate strengths and their estimates according to (i) the proposals of Young (2004) and Silvestre *et al*. (2013), and (ii) the developed DSM-F procedure (dimensions in *mm*, stresses in *MPa*)

		Buckling analysis					Test	Young (2004)	Silvestre *et al*. (2013)		Proposed DSM-F Procedure				
Section	L	f_{crft}	f_{cre}	f_{crf}	f_{crt}	f_y	f_u	f_u/f_p	f_{nle}	f_u/f_{nle}	Δ_f	a	b	f_{nfte}	f_u/f_{nfte}
Popovic *et al.* (1999) 50x2.5	150	359.7	38074.4	152297.5	360.0	396	308	1.30	329.3	0.94	0.09	0.42	0.17	320.9	0.96
	550	196.4	2832.0	11327.9	197.7	396	225	1.01	249.5	0.90	0.66	0.54	0.24	219.8	1.02
	970	185.1	910.5	3641.9	188.8	396	173	0.90	213.6	0.81	2.01	0.74	0.22	184.7	0.94
	1379	179.3	450.5	1802.0	186.7	396	154	1.00	172.3	0.89	4.14	0.90	0.24	156.6	0.98
	1747	173.9	280.7	1122.8	185.9	396	130	1.11	133.2	0.98	6.87	0.90	0.25	142.1	0.92
	2199	166.3	177.2	708.6	185.4	396	110	1.44	88.6	1.24	11.50	0.91	0.25	121.6	0.90
	2598	158.3	126.9	507.7	185.2	396	93	1.70	63.0	1.23	16.99	0.92	0.25	101.0	0.92
Popovic *et al.* (1999) 50x4.0	150	918.4	38825.9	155303.7	920.4	388	424	1.26	385.3	1.10	0.22	0.45	0.20	386.4	1.10
	970	458.4	928.5	3713.8	482.6	388	314	1.19	286.2	1.10	5.28	0.90	0.25	293.6	1.07
	1381	428.2	458.1	1832.2	477.2	388	250	1.33	215.7	1.16	11.44	0.91	0.25	256.9	0.97
	1743	396.8	287.5	1150.2	475.2	388	178	1.41	152.0	1.16	19.75	0.93	0.25	217.3	0.82
Popovic *et al.* (1999) 50x5.0	150	1366.9	37819.0	151276.2	1371.6	388	414	1.15	385.3	1.07	0.34	0.48	0.22	386.3	1.07
	970	663.3	904.4	3617.5	719.2	388	307	1.20	288.2	1.06	8.42	0.91	0.25	324.2	0.95
	1378	598.6	448.1	1792.5	711.1	388	216	1.21	213.0	1.02	18.80	0.93	0.25	270.1	0.80
	1749	528.7	278.2	1112.7	708.1	388	180	1.56	148.0	1.22	33.95	0.96	0.25	210.5	0.86
Young (2004) 70x1.2	250	36.3	28143.0	112571.9	36.4	550	143	1.16	176.9	0.81	0.01	0.40	0.15	176.0	0.81
	1000	22.3	1758.9	7035.7	22.3	550	113	1.03	127.8	0.88	0.12	0.43	0.18	123.0	0.92
	1500	21.7	781.7	3127.0	21.8	550	92	0.99	107.0	0.86	0.26	0.46	0.21	99.7	0.92
	2000	21.5	439.7	1758.9	21.6	550	76	1.04	84.1	0.90	0.46	0.51	0.23	77.4	0.98
	2500	21.3	281.4	1125.7	21.5	550	70	1.28	61.8	1.13	0.72	0.55	0.24	59.4	1.18
	3000	21.2	195.4	781.7	21.4	550	48	1.10	48.7	0.99	1.05	0.60	0.21	45.5	1.06
	3500	21.1	143.6	574.3	21.4	550	35	0.96	39.9	0.87	1.43	0.66	0.21	36.0	0.97
Young (2004) 70x1.5	250	59.2	27851.7	111406.6	59.2	530	189	1.26	208.4	0.90	0.02	0.40	0.16	206.6	0.91
	1000	36.3	1740.7	6962.9	36.4	530	148	1.12	151.3	0.98	0.20	0.45	0.20	140.2	1.05
	1500	35.4	773.7	3094.6	35.5	530	120	1.07	127.0	0.94	0.43	0.50	0.23	110.7	1.08
	2000	35.0	435.2	1740.7	35.2	530	83	0.93	100.3	0.83	0.77	0.56	0.24	86.5	0.96
	2500	34.7	278.5	1114.1	35.1	530	75	1.13	74.0	1.01	1.20	0.63	0.21	66.7	1.12
	3000	34.4	193.4	773.7	35.0	530	62	1.17	58.3	1.07	1.75	0.71	0.22	52.3	1.19
	3500	34.2	142.1	568.4	35.0	530	55	1.24	47.2	1.16	2.40	0.78	0.22	41.8	1.31
Young (2004) 72x2.0	250	93.5	28379.0	113515.9	93.5	500	212	1.22	237.2	0.90	0.03	0.41	0.16	234.2	0.91
	1000	57.0	1773.7	7094.7	57.1	500	180	1.15	173.9	1.03	0.30	0.47	0.21	154.9	1.16
	1500	55.4	788.3	3153.2	55.8	500	134	1.00	147.5	0.91	0.67	0.54	0.24	123.0	1.09
	2000	54.7	443.4	1773.7	55.3	500	102	0.94	118.1	0.86	1.19	0.63	0.21	97.0	1.05
	2500	54.1	283.8	1135.2	55.1	500	84	1.03	88.8	0.95	1.88	0.72	0.22	75.5	1.12
	3000	53.5	197.1	788.3	55.0	500	56	0.87	68.1	0.82	2.73	0.81	0.23	60.6	0.92
	3500	52.9	144.8	579.2	54.9	500	54	1.03	55.4	0.98	3.77	0.89	0.24	51.9	1.04
Mesacasa Jr. (2011) 60x2.0	400	101.8	7411.3	29608.8	101.9	350	177	1.16	191.0	0.93	0.13	0.43	0.18	182.3	0.97
	600	92.5	3293.9	13159.5	92.8	350	166	1.11	179.3	0.93	0.27	0.46	0.21	163.8	1.01
	900	88.2	1464.0	5848.7	88.7	350	137	0.97	165.9	0.83	0.57	0.53	0.24	142.3	0.96
	1200	86.4	823.5	3289.9	87.3	350	128	0.97	151.6	0.85	1.01	0.60	0.21	126.8	1.01
	1800	84.3	366.0	1462.2	86.3	350	88	0.83	118.4	0.74	2.30	0.77	0.22	95.9	0.92
							Mean	1.14		0.98					1.00
							Sd. Dev.	0.18		0.15					0.11
							Max	1.70		1.24					1.31
							Min	0.83		0.74					0.80

ANNEX C: PIN-ENDED COLUMN EXPERIMENTAL DATA

Table C: Pin-ended column experimental ultimate strengths and their estimates according to (i) the proposals of Rasmussen (2006) and Silvestre *et al.* (2013), and (ii) the developed DSM-P procedure (dimensions in *mm*, stresses in *MPa*)

		Buckling analysis					Test	Rasmussen (2006)	Silvestre *et al.* (2013)		Proposed DSM-P Procedure							
Section	L	f_{crft}	f_{cre}	f_{crf}	f_{crt}	f_y	f_u	f_u/f_p	f_{nle}	f_u/f_{nle}	Δ_f	a	b	c	d	β	f_{nfte}	f_u/f_{nfte}
Wilhoite *et al.* (1984) 70x3.0	823	155.5	595.7	9388.6	156.5	465	174.3	1.18	133.8	1.30	0.63	0.54	0.24	0.41	0.85	0.69	128.9	1.35
	823	155.5	595.7	9388.6	156.5	465	174.3	1.18	133.8	1.30	0.63	0.54	0.24	0.41	0.85	0.69	128.9	1.35
	1227	149.5	268.0	4223.9	151.6	465	140.1	1.27	109.7	1.28	1.38	0.65	0.21	0.31	0.90	0.76	110.1	1.27
	1227	149.5	268.0	4223.9	151.6	465	144.5	1.30	109.7	1.32	1.38	0.65	0.21	0.31	0.90	0.76	110.1	1.31
	1227	149.5	268.0	4223.9	151.6	465	156.3	1.41	109.7	1.42	1.38	0.65	0.21	0.31	0.90	0.76	110.1	1.42
	1636	146.2	150.8	2375.9	149.8	465	116.3	1.48	75.4	1.54	2.46	0.79	0.22	0.16	0.98	0.86	93.1	1.25
	1636	146.2	150.8	2375.9	149.8	465	125.2	1.59	75.4	1.66	2.46	0.79	0.22	0.16	0.98	0.86	93.1	1.35
	1636	146.2	150.8	2375.9	149.8	465	142.3	1.81	75.4	1.89	2.46	0.79	0.22	0.16	0.98	0.86	93.1	1.53
Popovic *et al.* (1999) 50x2.5	286	232.4	2618.3	41893.2	232.9	396	187.0	1.06	197.6	0.95	0.21	0.45	0.20	0.46	0.82	0.88	224.3	0.83
	285	232.7	2636.7	42187.7	233.2	396	211.7	1.07	197.9	1.07	0.21	0.45	0.20	0.46	0.82	0.88	224.8	0.94
	490	200.0	892.0	14271.9	201.0	396	157.8	1.07	166.7	0.95	0.53	0.52	0.24	0.42	0.84	0.82	170.6	0.93
	490	200.0	892.0	14271.9	201.0	396	179.8	1.03	166.7	1.08	0.53	0.52	0.24	0.42	0.84	0.82	170.6	1.05
	674	191.4	471.4	7543.2	193.3	396	138.6	1.13	150.6	0.92	0.98	0.59	0.21	0.37	0.87	0.83	154.7	0.90
	675	191.4	470.1	7520.9	193.3	396	213.0	1.42	150.4	1.42	0.98	0.59	0.21	0.36	0.87	0.83	153.3	1.39
	900	186.3	264.4	4230.5	189.5	396	112.6	1.19	124.6	0.90	1.73	0.70	0.22	0.26	0.93	0.86	133.3	0.84
	900	186.3	264.4	4230.5	189.5	396	143.9	1.21	124.6	1.16	1.73	0.70	0.22	0.26	0.93	0.86	133.3	1.08
	1099	183.1	177.3	2837.1	187.9	396	79.4	1.06	89.0	0.89	2.59	0.80	0.23	0.00	1.07	0.71	92.3	0.86
	1100	183.1	177.0	2832.0	187.9	396	110.8	1.14	88.0	1.11	2.59	0.80	0.23	0.00	1.07	0.71	92.1	1.20
Popovic *et al.* (1999) 50x4.0	285	593.1	2688.8	43020.4	596.2	388	367.1	1.15	344.4	1.07	0.52	0.52	0.24	0.41	0.85	1.00	328.8	1.12
	490	507.1	909.6	14553.7	514.0	388	294.9	1.00	285.0	1.03	1.35	0.65	0.21	0.31	0.90	1.00	311.3	0.95
	675	482.0	479.3	7669.3	494.1	388	205.3	0.78	88.0	0.93	2.51	0.79	0.23	0.00	1.07	0.89	247.1	0.83
Popovic *et al.* (1999) 50x5.0	285	881.2	2619.0	41904.8	888.3	388	360.0	0.99	350.1	1.03	0.81	0.57	0.23	0.37	0.87	1.00	364.7	0.99
	490	750.1	886.0	14176.2	765.8	388	277.0	0.86	286.4	0.97	2.10	0.75	0.22	0.20	0.96	1.00	323.0	0.86
	490	750.1	886.0	14176.2	765.8	388	272.8	0.85	286.4	0.95	2.10	0.75	0.22	0.20	0.96	1.00	323.0	0.84
	675	708.4	466.9	7470.4	736.2	388	213.7	0.78	218.0	0.98	3.93	0.89	0.24	0.00	1.12	0.88	239.6	0.89
	675	708.4	466.9	7470.4	736.2	388	195.6	0.85	218.0	0.89	3.93	0.89	0.24	0.00	1.12	0.88	239.6	0.82
Chodraui *et al.* (2006) 60x2.4	480	141.3	1306.7	20870.1	141.6	371	111.9	0.82	126.1	0.89	0.26	0.46	0.21	0.46	0.82	0.69	133.7	0.84
	835	129.5	431.8	6896.6	130.4	371	104.7	0.91	109.4	0.96	0.72	0.55	0.24	0.40	0.85	0.71	105.6	0.99
	1195	125.8	210.8	3367.2	127.6	371	83.0	0.91	89.8	0.92	1.46	0.67	0.21	0.29	0.91	0.78	91.3	0.91
	1550	123.5	125.3	2001.4	126.5	371	75.8	1.14	62.7	1.21	2.47	0.79	0.22	0.15	0.99	0.86	77.9	0.97
Maia *et al.* (2008) 60x2.4	480	142.6	1319.5	21075.7	143.0	357	111.9	0.82	126.7	0.88	0.26	0.46	0.21	0.46	0.82	0.71	135.0	0.83
	650	134.7	719.6	11493.1	135.3	357	130.3	1.02	117.5	1.11	0.44	0.50	0.23	0.45	0.83	0.72	119.5	1.09
	835	130.8	436.0	6964.5	131.7	357	104.7	0.91	110.1	0.95	0.72	0.55	0.24	0.40	0.85	0.73	106.9	0.98
	1195	127.0	212.9	3400.4	128.9	357	81.2	0.88	91.0	0.89	1.46	0.67	0.21	0.29	0.91	0.79	92.5	0.88
	1450	125.3	144.6	2309.6	128.0	357	75.8	1.02	71.0	1.07	2.15	0.76	0.22	0.19	0.97	0.84	82.1	0.92
							Mean	1.09		1.12							Mean	1.10
							Sd. Dev.	0.24		0.25							Sd. Dev	0.11
							Max	1.81		1.89							Max.	1.74
							Min	0.72		0.88							Min	0.96

ANNEX D: FIXED-ENDED COLUMN NUMERICAL DATA

Table D: Fixed-ended column numerical ultimate strengths and their estimates according to (i) the proposal of Silvestre *et al.* (2013), and (ii) the developed DSM-F procedure (dimensions in *mm*, stresses in *MPa*)

		Buckling analysis					Numerical	Silvestre *et al.* (2013)		Proposed DSM-F Procedure				
Section	L	f_{crft}	f_{cre}	f_{crf}	f_{crt}	f_y	f_u	f_{nle}	f_u/f_{nle}	Δ_f	a	b	f_{nfte}	f_u/f_{nfte}
70x1.2	532	27.2	5983.7	23922.2	27.3	30	26.6	24.7	1.08	0.04	0.41	0.16	24.4	1.11
	980	24.7	1763.4	7049.7	24.8	30	25.4	23.8	1.07	0.13	0.43	0.18	22.9	1.09
	1330	24.2	957.4	3827.5	24.3	30	24.5	23.4	1.05	0.24	0.46	0.20	22.0	1.09
	1820	23.9	511.3	2044.0	24.0	30	23.4	23.0	1.02	0.44	0.50	0.23	20.9	1.10
	2520	23.7	266.7	1066.2	23.9	30	22.1	22.4	0.99	0.85	0.57	0.23	20.4	1.08
	3640	23.4	127.8	511.0	23.8	30	21.4	21.1	1.02	1.80	0.71	0.22	19.6	1.07
	4200	23.2	96.0	383.8	23.8	30	19.3	20.3	0.95	2.42	0.78	0.22	19.0	1.00
	5320	22.9	59.8	239.2	23.8	30	18.0	18.5	0.97	3.96	0.90	0.24	17.8	1.01
	7000	22.2	34.6	138.2	23.8	30	14.8	15.4	0.96	7.17	0.90	0.25	16.2	0.92
	8900	21.1	21.4	85.5	23.7	30	11.3	11.3	1.00	12.32	0.91	0.25	14.3	0.79
	532	27.2	5983.7	23922.2	27.3	60	36.7	38.9	0.94	0.04	0.41	0.16	38.4	0.96
	980	24.7	1763.4	7049.7	24.8	60	33.6	37.1	0.90	0.13	0.43	0.18	35.6	0.96
	1330	24.2	957.4	3827.5	24.3	60	31.6	36.4	0.87	0.24	0.46	0.20	33.8	0.95
	1820	23.9	511.3	2044.0	24.0	60	28.9	35.3	0.82	0.44	0.50	0.23	31.4	0.92
	2520	23.7	266.7	1066.2	23.9	60	25.3	33.5	0.75	0.85	0.57	0.23	29.0	0.86
	3640	23.4	127.8	511.0	23.8	60	24.1	29.9	0.81	1.80	0.71	0.22	25.3	0.95
	4200	23.2	96.0	383.8	23.8	60	20.6	27.8	0.74	2.42	0.78	0.22	23.4	0.90
	5320	22.9	59.8	239.2	23.8	60	19.3	23.3	0.83	3.96	0.90	0.24	20.6	0.92
	7000	22.2	34.6	138.2	23.8	60	14.8	16.4	0.90	7.17	0.90	0.25	18.3	0.82
	8900	21.1	21.4	85.5	23.7	60	12.0	10.7	1.12	12.32	0.91	0.25	15.1	0.87
	532	27.2	5983.7	23922.2	27.3	120	64.5	60.5	1.07	0.04	0.41	0.16	59.5	1.09
	980	24.7	1763.4	7049.7	24.8	120	52.8	57.1	0.93	0.13	0.43	0.18	54.2	0.98
	1330	24.2	957.4	3827.5	24.3	120	54.0	55.2	0.98	0.24	0.46	0.20	50.5	1.07
	1820	23.9	511.3	2044.0	24.0	120	47.7	52.3	0.91	0.44	0.50	0.23	45.4	1.06
	2520	23.7	266.7	1066.2	23.9	120	39.7	47.4	0.84	0.85	0.57	0.23	39.3	1.02
	3640	23.4	127.8	511.0	23.8	120	31.3	38.0	0.82	1.80	0.71	0.22	30.4	1.02
	4200	23.2	96.0	383.8	23.8	120	24.1	32.9	0.73	2.42	0.78	0.22	26.8	0.89
	5320	22.9	59.8	239.2	23.8	120	21.2	23.3	0.91	3.96	0.90	0.24	22.0	0.95
	7000	22.2	34.6	138.2	23.8	120	14.8	15.9	0.93	7.17	0.90	0.25	18.6	0.81
	8900	21.1	21.4	85.5	23.7	120	12.0	10.7	1.12	12.32	0.91	0.25	15.1	0.87
	532	27.2	5983.7	23922.2	27.3	235	105.0	91.8	1.14	0.04	0.41	0.16	90.1	1.17
	980	24.7	1763.4	7049.7	24.8	235	85.0	84.8	1.00	0.13	0.43	0.18	80.2	1.06
	1330	24.2	957.4	3827.5	24.3	235	80.4	80.1	1.00	0.24	0.46	0.20	72.8	1.10
	1820	23.9	511.3	2044.0	24.0	235	68.8	72.6	0.95	0.44	0.50	0.23	62.3	1.11
	2520	23.7	266.7	1066.2	23.9	235	54.2	60.1	0.90	0.85	0.57	0.23	49.8	1.08
	3640	23.4	127.8	511.0	23.8	235	39.9	39.2	1.02	1.80	0.71	0.22	33.7	1.19
	4200	23.2	96.0	383.8	23.8	235	29.7	31.9	0.93	2.42	0.78	0.22	28.2	1.06
	5320	22.9	59.8	239.2	23.8	235	23.2	23.3	1.00	3.96	0.90	0.24	22.1	1.04
	7000	22.2	34.6	138.2	23.8	235	14.8	15.9	0.93	7.17	0.90	0.25	18.6	0.81
	8900	21.1	21.4	85.5	23.7	235	12.0	10.7	1.12	12.32	0.91	0.25	15.1	0.87
	532	27.2	5983.7	23922.2	27.3	400	142.0	126.4	1.12	0.04	0.41	0.16	124.1	1.14
	980	24.7	1763.4	7049.7	24.8	400	101.0	113.5	0.89	0.13	0.43	0.18	107.7	0.94
	1330	24.2	957.4	3827.5	24.3	400	93.3	103.6	0.90	0.24	0.46	0.20	94.9	0.98
	1820	23.9	511.3	2044.0	24.0	400	82.6	88.0	0.94	0.44	0.50	0.23	77.1	1.08
	2520	23.7	266.7	1066.2	23.9	400	63.1	64.1	0.98	0.85	0.57	0.23	56.6	1.11
	3640	23.4	127.8	511.0	23.8	400	43.1	38.5	1.12	1.80	0.71	0.22	34.1	1.26
	4200	23.2	96.0	383.8	23.8	400	30.3	31.9	0.95	2.42	0.78	0.22	28.2	1.06

Section	L	f_{crft}	f_{cre}	f_{crf}	f_{crt}	f_y	f_u	f_{nle}	f_u/f_{nle}	Δ_f	a	b	f_{nfte}	f_u/f_{nfte}
70x1.2	5320	22.9	59.8	239.2	23.8	400	23.7	23.3	1.02	3.96	0.90	0.24	22.1	1.09
	7000	22.2	34.6	138.2	23.8	400	14.8	15.9	0.93	7.17	0.90	0.25	18.6	0.81
	8900	21.1	21.4	85.5	23.7	400	12.0	10.7	1.12	12.32	0.91	0.25	15.1	0.87
	532	27.2	5983.7	23922.2	27.3	500	155.0	144.2	1.07	0.04	0.41	0.16	141.7	1.09
	980	24.7	1763.4	7049.7	24.8	500	131.0	127.2	1.03	0.13	0.43	0.18	121.2	1.08
	1330	24.2	957.4	3827.5	24.3	500	99.5	113.8	0.87	0.24	0.46	0.20	105.2	0.95
	1820	23.9	511.3	2044.0	24.0	500	93.0	93.0	1.00	0.44	0.50	0.23	83.1	1.12
	2520	23.7	266.7	1066.2	23.9	500	65.3	62.7	1.04	0.85	0.57	0.23	58.4	1.11
	3640	23.4	127.8	511.0	23.8	500	43.8	38.5	1.14	1.80	0.71	0.22	34.1	1.29
	4200	23.2	96.0	383.8	23.8	500	30.3	31.9	0.95	2.42	0.78	0.22	28.2	1.06
	5320	22.9	59.8	239.2	23.8	500	23.8	23.3	1.02	3.96	0.90	0.24	22.1	1.09
	7000	22.2	34.6	138.2	23.8	500	14.8	15.9	0.93	7.17	0.90	0.25	18.6	0.81
	8900	21.1	21.4	85.5	23.7	500	12.0	10.7	1.12	12.32	0.91	0.25	15.1	0.87
50x1.2	1500	46.4	384.1	1535.3	47.0	120	52.8	64.0	0.82	1.17	0.62	0.21	55.2	0.96
	2000	45.8	216.1	863.6	46.8	120	46.8	57.1	0.82	2.10	0.75	0.22	48.0	0.98
	2500	45.2	138.3	552.7	46.7	120	42.2	49.3	0.86	3.34	0.86	0.23	42.4	0.99
	3000	44.5	96.0	383.8	46.6	120	36.6	41.1	0.89	4.91	0.90	0.25	39.0	0.95
	4000	42.6	54.0	215.9	46.6	120	29.1	26.6	1.09	9.23	0.91	0.25	33.3	0.87
	1500	46.4	384.1	1535.3	47.0	235	80.6	86.4	0.93	1.17	0.62	0.21	70.6	1.15
	2000	45.8	216.1	863.6	46.8	235	63.6	69.6	0.91	2.10	0.75	0.22	56.0	1.14
	2500	45.2	138.3	552.7	46.7	235	50.8	52.5	0.97	3.34	0.86	0.23	46.1	1.11
	3000	44.5	96.0	383.8	46.6	235	38.0	39.8	0.95	4.91	0.90	0.25	40.8	0.93
	4000	42.6	54.0	215.9	46.6	235	29.1	26.6	1.09	9.23	0.91	0.25	33.3	0.87
	1500	46.4	384.1	1535.3	47.0	400	100.0	100.4	1.00	1.17	0.62	0.21	82.2	1.22
	2000	45.8	216.1	863.6	46.8	400	73.4	69.7	1.05	2.10	0.75	0.22	59.9	1.22
	2500	45.2	138.3	552.7	46.7	400	55.3	51.0	1.09	3.34	0.86	0.23	46.6	1.18
	3000	44.5	96.0	383.8	46.6	400	38.9	39.8	0.98	4.91	0.90	0.25	40.8	0.96
	4000	42.6	54.0	215.9	46.6	400	29.1	26.6	1.09	9.23	0.91	0.25	33.3	0.87
	1500	46.4	384.1	1535.3	47.0	500	89.0	103.1	0.86	1.17	0.62	0.21	86.2	1.03
	2000	45.8	216.1	863.6	46.8	500	67.0	68.5	0.98	2.10	0.75	0.22	60.4	1.11
	2500	45.2	138.3	552.7	46.7	500	55.0	51.0	1.08	3.34	0.86	0.23	46.6	1.18
	3000	44.5	96.0	383.8	46.6	500	39.0	39.8	0.98	4.91	0.90	0.25	40.8	0.96
	4000	42.6	54.0	215.9	46.6	500	29.1	26.6	1.09	9.23	0.91	0.25	33.3	0.87
50x2.6	950	218.6	959.9	3827.5	223.6	120	111.0	110.0	1.01	2.27	0.77	0.22	113.9	0.97
	1500	208.2	385.0	1535.3	220.5	120	100.0	96.7	1.03	5.88	0.90	0.25	105.1	0.95
	2000	197.6	216.6	863.6	219.6	120	87.8	81.7	1.07	11.13	0.91	0.25	95.2	0.92
	950	218.6	959.9	3827.5	223.6	235	196.0	174.2	1.13	2.27	0.77	0.22	167.9	1.17
	1500	208.2	385.0	1535.3	220.5	235	176.0	144.4	1.22	5.88	0.90	0.25	147.9	1.19
	2000	197.6	216.6	863.6	219.6	235	128.0	110.8	1.16	11.13	0.91	0.25	130.9	0.98
	950	218.6	959.9	3827.5	223.6	400	220.0	229.5	0.96	2.27	0.77	0.22	203.2	1.08
	1500	208.2	385.0	1535.3	220.5	400	192.0	169.3	1.13	5.88	0.90	0.25	169.5	1.13
	2000	197.6	216.6	863.6	219.6	400	132.0	111.2	1.19	11.13	0.91	0.25	144.5	0.91
	950	218.6	959.9	3827.5	223.6	500	237.0	253.5	0.94	2.27	0.77	0.22	217.0	1.09
	1500	208.2	385.0	1535.3	220.5	500	193.0	174.3	1.11	5.88	0.90	0.25	175.7	1.10
	2000	197.6	216.6	863.6	219.6	500	152.0	108.3	1.40	11.13	0.91	0.25	146.2	1.04

Section	L	f_{crft}	f_{cre}	f_{crf}	f_{crt}	f_y	f_u	f_{nle}	f_u/f_{nle}	Δ_f	a	b	f_{nfte}	f_u/f_{nfte}
	1000	66.5	2801.0	11192.1	66.6	120	76.7	–	–	0.22	0.45	0.20	77.0	1.00
	1000	66.5	2801.0	11192.1	66.6	235	125	–	–	0.22	0.45	0.20	115.3	1.08
	1000	66.5	2801.0	11192.1	66.6	400	184	–	–	0.22	0.45	0.20	156.3	1.18
	1000	66.5	2801.0	11192.1	66.6	500	210	–	–	0.22	0.45	0.20	176.7	1.19
	1000	66.5	2801.0	11192.1	66.6	600	229	–	–	0.22	0.45	0.20	194.9	1.17
	1000	66.5	2801.0	11192.1	66.6	900	269	–	–	0.22	0.45	0.20	240.4	1.12
	1000	66.5	2801.0	11192.1	66.6	1200	321	–	–	0.22	0.45	0.20	276.6	1.16
	1200	65.1	1945.1	7772.3	65.3	120	74.4	–	–	0.32	0.48	0.22	74.1	1.00
	1200	65.1	1945.1	7772.3	65.3	235	121	–	–	0.32	0.48	0.22	109.6	1.10
	1200	65.1	1945.1	7772.3	65.3	400	174	–	–	0.32	0.48	0.22	146.3	1.19
	1200	65.1	1945.1	7772.3	65.3	500	190	–	–	0.32	0.48	0.22	164.2	1.16
	1200	65.1	1945.1	7772.3	65.3	600	207	–	–	0.32	0.48	0.22	179.9	1.15
	1200	65.1	1945.1	7772.3	65.3	900	238	–	–	0.32	0.48	0.22	218.0	1.09
	1200	65.1	1945.1	7772.3	65.3	1200	248	–	–	0.32	0.48	0.22	246.9	1.00
	1500	63.9	1244.9	4974.3	64.2	120	71.2	–	–	0.49	0.51	0.23	70.6	1.01
	1500	63.9	1244.9	4974.3	64.2	235	112	–	–	0.49	0.51	0.23	101.8	1.10
	1500	63.9	1244.9	4974.3	64.2	400	157	–	–	0.49	0.51	0.23	132.6	1.18
	1500	63.9	1244.9	4974.3	64.2	500	175	–	–	0.49	0.51	0.23	146.9	1.19
	1500	63.9	1244.9	4974.3	64.2	600	189	–	–	0.49	0.51	0.23	159.2	1.19
	1500	63.9	1244.9	4974.3	64.2	900	222	–	–	0.49	0.51	0.23	187.2	1.19
	1500	63.9	1244.9	4974.3	64.2	1200	245	–	–	0.49	0.51	0.23	206.5	1.19
90x2.5	2000	62.9	700.2	2798.0	63.4	120	67.1	–	–	0.86	0.58	0.23	67.2	1.00
	2000	62.9	700.2	2798.0	63.4	235	98	–	–	0.86	0.58	0.23	91.8	1.07
	2000	62.9	700.2	2798.0	63.4	400	130	–	–	0.86	0.58	0.23	113.5	1.14
	2000	62.9	700.2	2798.0	63.4	500	143	–	–	0.86	0.58	0.23	122.8	1.16
	2000	62.9	700.2	2798.0	63.4	600	152	–	–	0.86	0.58	0.23	130.1	1.17
	2000	62.9	700.2	2798.0	63.4	900	169	–	–	0.86	0.58	0.23	144.7	1.17
	2000	62.9	700.2	2798.0	63.4	1200	179	–	–	0.86	0.58	0.23	152.2	1.18
	2500	62.2	448.2	1790.7	63.0	120	62.6	–	–	1.35	0.65	0.21	64.0	0.98
	2500	62.2	448.2	1790.7	63.0	235	77.3	–	–	1.35	0.65	0.21	82.2	0.94
	2500	62.2	448.2	1790.7	63.0	400	102	–	–	1.35	0.65	0.21	96.2	1.06
	2500	62.2	448.2	1790.7	63.0	500	111	–	–	1.35	0.65	0.21	101.3	1.10
	2500	62.2	448.2	1790.7	63.0	600	117	–	–	1.35	0.65	0.21	105.0	1.11
	2500	62.2	448.2	1790.7	63.0	900	127	–	–	1.35	0.65	0.21	110.3	1.15
	2500	62.2	448.2	1790.7	63.0	1200	132	–	–	1.35	0.65	0.21	110.9	1.19
	3000	61.6	311.2	1243.6	62.8	120	59.6	–	–	1.95	0.73	0.22	59.9	1.00
	3000	61.6	311.2	1243.6	62.8	235	68.9	–	–	1.95	0.73	0.22	72.7	0.95
	3000	61.6	311.2	1243.6	62.8	400	85.7	–	–	1.95	0.73	0.22	80.8	1.06
	3000	61.6	311.2	1243.6	62.8	500	91.6	–	–	1.95	0.73	0.22	83.3	1.10
	3000	61.6	311.2	1243.6	62.8	600	95.5	–	–	1.95	0.73	0.22	84.6	1.13
	3000	61.6	311.2	1243.6	62.8	900	102	–	–	1.95	0.73	0.22	85.1	1.20
	3000	61.6	311.2	1243.6	62.8	1200	104	–	–	1.95	0.73	0.22	85.1	1.22
	4000	60.4	175.1	699.5	62.6	120	53.9	–	–	3.55	0.88	0.24	53.0	1.02
	4000	60.4	175.1	699.5	62.6	235	56.9	–	–	3.55	0.88	0.24	59.0	0.97
	4000	60.4	175.1	699.5	62.6	400	62	–	–	3.55	0.88	0.24	60.9	1.02
	4000	60.4	175.1	699.5	62.6	500	64.1	–	–	3.55	0.88	0.24	60.9	1.05
	4000	60.4	175.1	699.5	62.6	600	65.4	–	–	3.55	0.88	0.24	60.9	1.07
	4000	60.4	175.1	699.5	62.6	900	67.2	–	–	3.55	0.88	0.24	60.9	1.10
	4000	60.4	175.1	699.5	62.6	1200	67.5	–	–	3.55	0.88	0.24	60.9	1.11

Section	L	f_{crft}	f_{cre}	f_{crf}	f_{crt}	f_y	f_u	f_{nle}	f_u/f_{nle}	Δ_f	a	b	f_{nfte}	f_u/f_{nfte}
	5000	59.1	112.0	447.7	62.5	120	47.8	–	–	5.71	0.90	0.25	48.7	0.98
	5000	59.1	112.0	447.7	62.5	235	48.1	–	–	5.71	0.90	0.25	52.3	0.92
	5000	59.1	112.0	447.7	62.5	400	48.1	–	–	5.71	0.90	0.25	52.4	0.92
	5000	59.1	112.0	447.7	62.5	500	48.1	–	–	5.71	0.90	0.25	52.4	0.92
	5000	59.1	112.0	447.7	62.5	600	48.1	–	–	5.71	0.90	0.25	52.4	0.92
	5000	59.1	112.0	447.7	62.5	900	48.1	–	–	5.71	0.90	0.25	52.4	0.92
	5000	59.1	112.0	447.7	62.5	1200	48.1	–	–	5.71	0.90	0.25	52.4	0.92
	6000	57.5	77.8	310.9	62.4	120	41.8	–	–	8.52	0.91	0.25	44.7	0.93
	6000	57.5	77.8	310.9	62.4	235	41.8	–	–	8.52	0.91	0.25	46.0	0.91
90x2.5	6000	57.5	77.8	310.9	62.4	400	41.8	–	–	8.52	0.91	0.25	46.0	0.91
	6000	57.5	77.8	310.9	62.4	500	41.8	–	–	8.52	0.91	0.25	46.0	0.91
	6000	57.5	77.8	310.9	62.4	600	41.8	–	–	8.52	0.91	0.25	46.0	0.91
	6000	57.5	77.8	310.9	62.4	900	41.8	–	–	8.52	0.91	0.25	46.0	0.91
	6000	57.5	77.8	310.9	62.4	1200	41.8	–	–	8.52	0.91	0.25	46.0	0.91
	7000	55.7	57.2	228.4	62.4	120	36.5	–	–	12.09	0.91	0.25	40.0	0.91
	7000	55.7	57.2	228.4	62.4	235	36.5	–	–	12.09	0.91	0.25	40.1	0.91
	7000	55.7	57.2	228.4	62.4	400	36.5	–	–	12.09	0.91	0.25	40.1	0.91
	7000	55.7	57.2	228.4	62.4	500	36.5	–	–	12.09	0.91	0.25	40.1	0.91
	7000	55.7	57.2	228.4	62.4	600	36.5	–	–	12.09	0.91	0.25	40.1	0.91
	7000	55.7	57.2	228.4	62.4	900	36.5	–	–	12.09	0.91	0.25	40.1	0.91
	7000	55.7	57.2	228.4	62.4	1200	36.5	–	–	12.09	0.91	0.25	40.1	0.91
	700	78.7	3458.2	13817.4	78.9	120	80	–	–	0.21	0.45	0.20	79.4	1.01
	700	78.7	3458.2	13817.4	78.9	235	130	–	–	0.21	0.45	0.20	119.6	1.09
	700	78.7	3458.2	13817.4	78.9	400	196	–	–	0.21	0.45	0.20	162.8	1.20
	700	78.7	3458.2	13817.4	78.9	500	227	–	–	0.21	0.45	0.20	184.5	1.23
	700	78.7	3458.2	13817.4	78.9	600	247	–	–	0.21	0.45	0.20	203.9	1.21
	700	78.7	3458.2	13817.4	78.9	900	313	–	–	0.21	0.45	0.20	253.1	1.24
	700	78.7	3458.2	13817.4	78.9	1200	317	–	–	0.21	0.45	0.20	292.7	1.08
	800	77.2	2647.7	10579.0	77.5	120	78.5	–	–	0.28	0.47	0.21	77.4	1.01
	800	77.2	2647.7	10579.0	77.5	235	125	–	–	0.28	0.47	0.21	115.5	1.08
	800	77.2	2647.7	10579.0	77.5	400	184	–	–	0.28	0.47	0.21	155.7	1.18
	800	77.2	2647.7	10579.0	77.5	500	227	–	–	0.28	0.47	0.21	175.7	1.29
	800	77.2	2647.7	10579.0	77.5	600	231	–	–	0.28	0.47	0.21	193.4	1.19
70x2.0	800	77.2	2647.7	10579.0	77.5	900	273	–	–	0.28	0.47	0.21	237.4	1.15
	800	77.2	2647.7	10579.0	77.5	1200	321	–	–	0.28	0.47	0.21	272.0	1.18
	900	76.2	2092.0	8358.7	76.5	120	77.2	–	–	0.34	0.48	0.22	75.5	1.02
	900	76.2	2092.0	8358.7	76.5	235	124	–	–	0.34	0.48	0.22	111.6	1.11
	900	76.2	2092.0	8358.7	76.5	400	180	–	–	0.34	0.48	0.22	148.9	1.21
	900	76.2	2092.0	8358.7	76.5	500	198	–	–	0.34	0.48	0.22	167.1	1.18
	900	76.2	2092.0	8358.7	76.5	600	217	–	–	0.34	0.48	0.22	183.1	1.18
	900	76.2	2092.0	8358.7	76.5	900	247	–	–	0.34	0.48	0.22	222.1	1.11
	900	76.2	2092.0	8358.7	76.5	1200	265	–	–	0.34	0.48	0.22	251.9	1.05
	1000	75.4	1694.5	6770.5	75.7	120	75.9	–	–	0.42	0.50	0.23	73.8	1.03
	1000	75.4	1694.5	6770.5	75.7	235	111	–	–	0.42	0.50	0.23	107.9	1.03
	1000	75.4	1694.5	6770.5	75.7	400	161	–	–	0.42	0.50	0.23	142.4	1.13
	1000	75.4	1694.5	6770.5	75.7	500	180	–	–	0.42	0.50	0.23	158.9	1.13
	1000	75.4	1694.5	6770.5	75.7	600	195	–	–	0.42	0.50	0.23	173.3	1.13
	1000	75.4	1694.5	6770.5	75.7	900	233	–	–	0.42	0.50	0.23	207.4	1.12
	1000	75.4	1694.5	6770.5	75.7	1200	233	–	–	0.42	0.50	0.23	232.7	1.00

Section	L	f_{crft}	f_{cre}	f_{crf}	f_{crt}	f_y	f_u	f_{nle}	f_u/f_{nle}	Δ_f	a	b	f_{nfte}	f_u/f_{nfte}
	1500	73.4	753.1	3009.1	74.0	120	70.4	–	–	0.94	0.59	0.22	69.3	1.02
	1500	73.4	753.1	3009.1	74.0	235	91	–	–	0.94	0.59	0.22	94.3	0.97
	1500	73.4	753.1	3009.1	74.0	400	126	–	–	0.94	0.59	0.22	116.3	1.08
	1500	73.4	753.1	3009.1	74.0	500	140	–	–	0.94	0.59	0.22	125.7	1.11
	1500	73.4	753.1	3009.1	74.0	600	151	–	–	0.94	0.59	0.22	133.3	1.13
	1500	73.4	753.1	3009.1	74.0	900	170	–	–	0.94	0.59	0.22	148.6	1.14
	1500	73.4	753.1	3009.1	74.0	1200	180	–	–	0.94	0.59	0.22	157.0	1.15
	2000	72.2	423.6	1692.6	73.5	120	65.4	–	–	1.67	0.70	0.22	64.3	1.02
	2000	72.2	423.6	1692.6	73.5	235	77.4	–	–	1.67	0.70	0.22	80.7	0.96
	2000	72.2	423.6	1692.6	73.5	400	100	–	–	1.67	0.70	0.22	92.7	1.08
	2000	72.2	423.6	1692.6	73.5	500	109	–	–	1.67	0.70	0.22	97.0	1.12
	2000	72.2	423.6	1692.6	73.5	600	116	–	–	1.67	0.70	0.22	99.9	1.16
	2000	72.2	423.6	1692.6	73.5	900	125	–	–	1.67	0.70	0.22	103.9	1.20
	2000	72.2	423.6	1692.6	73.5	1200	130	–	–	1.67	0.70	0.22	104.0	1.25
	2500	71.3	271.1	1083.3	73.2	120	61.3	–	–	2.64	0.81	0.23	59.2	1.03
	2500	71.3	271.1	1083.3	73.2	235	67.3	–	–	2.64	0.81	0.23	69.3	0.97
	2500	71.3	271.1	1083.3	73.2	400	80.9	–	–	2.64	0.81	0.23	74.9	1.08
	2500	71.3	271.1	1083.3	73.2	500	85.7	–	–	2.64	0.81	0.23	76.2	1.12
	2500	71.3	271.1	1083.3	73.2	600	88.8	–	–	2.64	0.81	0.23	76.8	1.16
	2500	71.3	271.1	1083.3	73.2	900	94	–	–	2.64	0.81	0.23	76.8	1.22
70x2.0	2500	71.3	271.1	1083.3	73.2	1200	95.8	–	–	2.64	0.81	0.23	76.8	1.25
	3000	70.3	188.3	752.3	73.0	120	57.4	–	–	3.87	0.89	0.24	55.1	1.04
	3000	70.3	188.3	752.3	73.0	235	60.5	–	–	3.87	0.89	0.24	61.4	0.99
	3000	70.3	188.3	752.3	73.0	400	65.9	–	–	3.87	0.89	0.24	63.7	1.04
	3000	70.3	188.3	752.3	73.0	500	68.2	–	–	3.87	0.89	0.24	63.7	1.07
	3000	70.3	188.3	752.3	73.0	600	69.8	–	–	3.87	0.89	0.24	63.7	1.10
	3000	70.3	188.3	752.3	73.0	900	71.9	–	–	3.87	0.89	0.24	63.7	1.13
	3000	70.3	188.3	752.3	73.0	1200	72.4	–	–	3.87	0.89	0.24	63.7	1.14
	3500	69.2	138.3	552.7	72.9	120	53.4	–	–	5.37	0.90	0.25	52.4	1.02
	3500	69.2	138.3	552.7	72.9	235	54.5	–	–	5.37	0.90	0.25	57.4	0.95
	3500	69.2	138.3	552.7	72.9	400	55.9	–	–	5.37	0.90	0.25	58.1	0.96
	3500	69.2	138.3	552.7	72.9	500	56.4	–	–	5.37	0.90	0.25	58.1	0.97
	3500	69.2	138.3	552.7	72.9	600	56.7	–	–	5.37	0.90	0.25	58.1	0.98
	3500	69.2	138.3	552.7	72.9	900	56.8	–	–	5.37	0.90	0.25	58.1	0.98
	3500	69.2	138.3	552.7	72.9	1200	56.8	–	–	5.37	0.90	0.25	58.1	0.98
	4000	68.0	105.9	423.2	72.9	120	49.5	–	–	7.18	0.90	0.25	49.9	0.99
	4000	68.0	105.9	423.2	72.9	235	49.4	–	–	7.18	0.90	0.25	53.4	0.93
	4000	68.0	105.9	423.2	72.9	400	49.4	–	–	7.18	0.90	0.25	53.4	0.93
	4000	68.0	105.9	423.2	72.9	500	49.4	–	–	7.18	0.90	0.25	53.4	0.93
	4000	68.0	105.9	423.2	72.9	600	49.4	–	–	7.18	0.90	0.25	53.4	0.93
	4000	68.0	105.9	423.2	72.9	900	49.4	–	–	7.18	0.90	0.25	53.4	0.93
	4000	68.0	105.9	423.2	72.9	1200	49.4	–	–	7.18	0.90	0.25	53.4	0.93
	4500	66.6	83.7	334.3	72.8	120	45.1	–	–	9.33	0.91	0.25	47.2	0.96
	4500	66.6	83.7	334.3	72.8	235	45.1	–	–	9.33	0.91	0.25	49.0	0.92
	4500	66.6	83.7	334.3	72.8	400	45.1	–	–	9.33	0.91	0.25	49.0	0.92
	4500	66.6	83.7	334.3	72.8	500	45.1	–	–	9.33	0.91	0.25	49.0	0.92
	4500	66.6	83.7	334.3	72.8	600	45.1	–	–	9.33	0.91	0.25	49.0	0.92
	4500	66.6	83.7	334.3	72.8	900	45.1	–	–	9.33	0.91	0.25	49.0	0.92
	4500	66.6	83.7	334.3	72.8	1200	45.1	–	–	9.33	0.91	0.25	49.0	0.92

Section	L	f_{crft}	f_{cre}	f_{crf}	f_{crt}	f_y	f_u	f_{nle}	f_u/f_{nle}	Δ_f	a	b	f_{nfte}	f_u/f_{nfte}
	5000	65.1	67.8	270.8	72.8	120	41.2	–	–	11.86	0.91	0.25	44.1	0.93
	5000	65.1	67.8	270.8	72.8	235	41.2	–	–	11.86	0.91	0.25	44.8	0.92
	5000	65.1	67.8	270.8	72.8	400	41.2	–	–	11.86	0.91	0.25	44.8	0.92
	5000	65.1	67.8	270.8	72.8	500	41.2	–	–	11.86	0.91	0.25	44.8	0.92
	5000	65.1	67.8	270.8	72.8	600	41.2	–	–	11.86	0.91	0.25	44.8	0.92
	5000	65.1	67.8	270.8	72.8	900	41.2	–	–	11.86	0.91	0.25	44.8	0.92
70x2.0	5000	65.1	67.8	270.8	72.8	1200	41.2	–	–	11.86	0.91	0.25	44.8	0.92
	5360	63.9	59.0	235.7	72.8	120	38.4	–	–	13.95	0.92	0.25	41.7	0.92
	5360	63.9	59.0	235.7	72.8	235	38.4	–	–	13.95	0.92	0.25	41.9	0.92
	5360	63.9	59.0	235.7	72.8	400	38.4	–	–	13.95	0.92	0.25	41.9	0.92
	5360	63.9	59.0	235.7	72.8	500	38.4	–	–	13.95	0.92	0.25	41.9	0.92
	5360	63.9	59.0	235.7	72.8	600	38.4	–	–	13.95	0.92	0.25	41.9	0.92
	5360	63.9	59.0	235.7	72.8	900	38.4	–	–	13.95	0.92	0.25	41.9	0.92
	5360	63.9	59.0	235.7	72.8	1200	38.4	–	–	13.95	0.92	0.25	41.9	0.92
	800	52.8	1944.8	7772.3	52.9	120	67.4	–	–	0.26	0.46	0.21	69.5	0.97
	800	52.8	1944.8	7772.3	52.9	235	109	–	–	0.26	0.46	0.21	102.8	1.06
	800	52.8	1944.8	7772.3	52.9	400	157	–	–	0.26	0.46	0.21	137.7	1.14
	800	52.8	1944.8	7772.3	52.9	500	176	–	–	0.26	0.46	0.21	154.7	1.14
	800	52.8	1944.8	7772.3	52.9	600	190	–	–	0.26	0.46	0.21	169.7	1.12
	800	52.8	1944.8	7772.3	52.9	900	234	–	–	0.26	0.46	0.21	206.3	1.13
	800	52.8	1944.8	7772.3	52.9	1200	274	–	–	0.26	0.46	0.21	234.2	1.17
	900	52.2	1536.7	6141.1	52.4	120	64.1	–	–	0.32	0.48	0.22	67.7	0.95
	900	52.2	1536.7	6141.1	52.4	235	96.8	–	–	0.32	0.48	0.22	99.0	0.98
	900	52.2	1536.7	6141.1	52.4	400	137	–	–	0.32	0.48	0.22	131.1	1.05
	900	52.2	1536.7	6141.1	52.4	500	150	–	–	0.32	0.48	0.22	146.4	1.02
	900	52.2	1536.7	6141.1	52.4	600	161	–	–	0.32	0.48	0.22	159.8	1.01
	900	52.2	1536.7	6141.1	52.4	900	184	–	–	0.32	0.48	0.22	191.5	0.96
	900	52.2	1536.7	6141.1	52.4	1200	205	–	–	0.32	0.48	0.22	214.7	0.96
60x1.5	1000	51.8	1244.7	4974.3	52.0	120	62	–	–	0.39	0.49	0.23	65.9	0.94
	1000	51.8	1244.7	4974.3	52.0	235	87.1	–	–	0.39	0.49	0.23	95.3	0.91
	1000	51.8	1244.7	4974.3	52.0	400	137	–	–	0.39	0.49	0.23	124.5	1.10
	1000	51.8	1244.7	4974.3	52.0	500	152	–	–	0.39	0.49	0.23	138.3	1.10
	1000	51.8	1244.7	4974.3	52.0	600	164	–	–	0.39	0.49	0.23	150.0	1.09
	1000	51.8	1244.7	4974.3	52.0	900	197	–	–	0.39	0.49	0.23	177.0	1.11
	1000	51.8	1244.7	4974.3	52.0	1200	222	–	–	0.39	0.49	0.23	195.8	1.13
	1500	50.7	553.2	2210.8	51.2	120	54.1	–	–	0.88	0.58	0.23	60.1	0.90
	1500	50.7	553.2	2210.8	51.2	235	78.9	–	–	0.88	0.58	0.23	80.6	0.98
	1500	50.7	553.2	2210.8	51.2	400	106	–	–	0.88	0.58	0.23	98.1	1.08
	1500	50.7	553.2	2210.8	51.2	500	116	–	–	0.88	0.58	0.23	105.1	1.10
	1500	50.7	553.2	2210.8	51.2	600	122	–	–	0.88	0.58	0.23	110.5	1.10
	1500	50.7	553.2	2210.8	51.2	900	133	–	–	0.88	0.58	0.23	120.0	1.11
	1500	50.7	553.2	2210.8	51.2	1200	138	–	–	0.88	0.58	0.23	123.4	1.12
	2000	50.1	331.2	1243.6	50.9	120	50	–	–	1.57	0.68	0.22	54.7	0.91
	2000	50.1	331.2	1243.6	50.9	235	65	–	–	1.57	0.68	0.22	67.6	0.96
	2000	50.1	331.2	1243.6	50.9	400	82	–	–	1.57	0.68	0.22	76.4	1.07
	2000	50.1	331.2	1243.6	50.9	500	87.4	–	–	1.57	0.68	0.22	79.2	1.10
	2000	50.1	331.2	1243.6	50.9	600	90.9	–	–	1.57	0.68	0.22	80.8	1.12
	2000	50.1	331.2	1243.6	50.9	900	96.5	–	–	1.57	0.68	0.22	81.8	1.18
	2000	50.1	331.2	1243.6	50.9	1200	98.4	–	–	1.57	0.68	0.22	81.8	1.20

Section	L	f_{crft}	f_{cre}	f_{crf}	f_{crt}	f_y	f_u	f_{nle}	f_u/f_{nle}	Δ_f	a	b	f_{nfte}	f_u/f_{nfte}
	2500	49.5	199.2	795.9	50.7	120	46.4	–	–	2.49	0.79	0.22	48.8	0.95
	2500	49.5	199.2	795.9	50.7	235	54.3	–	–	2.49	0.79	0.22	55.8	0.97
	2500	49.5	199.2	795.9	50.7	400	63.7	–	–	2.49	0.79	0.22	58.9	1.08
	2500	49.5	199.2	795.9	50.7	500	66.4	–	–	2.49	0.79	0.22	59.1	1.12
	2500	49.5	199.2	795.9	50.7	600	68.2	–	–	2.49	0.79	0.22	59.1	1.15
	2500	49.5	199.2	795.9	50.7	900	70.8	–	–	2.49	0.79	0.22	59.1	1.20
	2500	49.5	199.2	795.9	50.7	1200	71.3	–	–	2.49	0.79	0.22	59.1	1.21
	3000	48.9	138.3	552.7	50.7	120	42.9	–	–	3.64	0.88	0.24	44.4	0.97
	3000	48.9	138.3	552.7	50.7	235	46	–	–	3.64	0.88	0.24	48.2	0.95
	3000	48.9	138.3	552.7	50.7	400	50.3	–	–	3.64	0.88	0.24	48.7	1.03
	3000	48.9	138.3	552.7	50.7	500	51.6	–	–	3.64	0.88	0.24	48.7	1.06
	3000	48.9	138.3	552.7	50.7	600	52.4	–	–	3.64	0.88	0.24	48.7	1.08
	3000	48.9	138.3	552.7	50.7	900	53.1	–	–	3.64	0.88	0.24	48.7	1.09
	3000	48.9	138.3	552.7	50.7	1200	53.2	–	–	3.64	0.88	0.24	48.7	1.09
	3500	48.2	101.6	406.1	50.6	120	39.3	–	–	5.05	0.90	0.25	41.7	0.94
	3500	48.2	101.6	406.1	50.6	235	40.3	–	–	5.05	0.90	0.25	43.9	0.92
	3500	48.2	101.6	406.1	50.6	400	41.2	–	–	5.05	0.90	0.25	43.9	0.94
	3500	48.2	101.6	406.1	50.6	500	41.4	–	–	5.05	0.90	0.25	43.9	0.94
	3500	48.2	101.6	406.1	50.6	600	41.5	–	–	5.05	0.90	0.25	43.9	0.94
	3500	48.2	101.6	406.1	50.6	900	41.5	–	–	5.05	0.90	0.25	43.9	0.94
60x1.5	3500	48.2	101.6	406.1	50.6	1200	41.5	–	–	5.05	0.90	0.25	43.9	0.94
	4000	47.4	77.8	310.9	50.6	120	36.3	–	–	6.74	0.90	0.25	39.3	0.92
	4000	47.4	77.8	310.9	50.6	235	36.3	–	–	6.74	0.90	0.25	40.3	0.90
	4000	47.4	77.8	310.9	50.6	400	36.3	–	–	6.74	0.90	0.25	40.3	0.90
	4000	47.4	77.8	310.9	50.6	500	36.3	–	–	6.74	0.90	0.25	40.3	0.90
	4000	47.4	77.8	310.9	50.6	600	36.3	–	–	6.74	0.90	0.25	40.3	0.90
	4000	47.4	77.8	310.9	50.6	900	36.3	–	–	6.74	0.90	0.25	40.3	0.90
	4000	47.4	77.8	310.9	50.6	1200	36.3	–	–	6.74	0.90	0.25	40.3	0.90
	4500	46.5	61.5	245.6	50.6	120	32.8	–	–	8.75	0.91	0.25	36.7	0.89
	4500	46.5	61.5	245.6	50.6	235	32.8	–	–	8.75	0.91	0.25	36.9	0.89
	4500	46.5	61.5	245.6	50.6	400	32.8	–	–	8.75	0.91	0.25	36.9	0.89
	4500	46.5	61.5	245.6	50.6	500	32.8	–	–	8.75	0.91	0.25	36.9	0.89
	4500	46.5	61.5	245.6	50.6	600	32.8	–	–	8.75	0.91	0.25	36.9	0.89
	4500	46.5	61.5	245.6	50.6	900	32.8	–	–	8.75	0.91	0.25	36.9	0.89
	4500	46.5	61.5	245.6	50.6	1200	32.8	–	–	8.75	0.91	0.25	36.9	0.89
	5000	45.5	49.8	199.0	50.5	120	29.4	–	–	11.11	0.91	0.25	33.6	0.87
	5000	45.5	49.8	199.0	50.5	235	29.4	–	–	11.11	0.91	0.25	33.6	0.87
	5000	45.5	49.8	199.0	50.5	400	29.4	–	–	11.11	0.91	0.25	33.6	0.87
	5000	45.5	49.8	199.0	50.5	500	29.4	–	–	11.11	0.91	0.25	33.6	0.87
	5000	45.5	49.8	199.0	50.5	600	29.4	–	–	11.11	0.91	0.25	33.6	0.87
	5000	45.5	49.8	199.0	50.5	900	29.4	–	–	11.11	0.91	0.25	33.6	0.87
	5000	45.5	49.8	199.0	50.5	1200	29.4	–	–	11.11	0.91	0.25	33.6	0.87
	5260	44.9	45.0	179.8	50.5	120	28	–	–	12.49	0.91	0.25	32.0	0.88
	5260	44.9	45.0	179.8	50.5	235	28	–	–	12.49	0.91	0.25	32.0	0.88
	5260	44.9	45.0	179.8	50.5	400	28	–	–	12.49	0.91	0.25	32.0	0.88
	5260	44.9	45.0	179.8	50.5	500	28	–	–	12.49	0.91	0.25	32.0	0.88
	5260	44.9	45.0	179.8	50.5	600	28	–	–	12.49	0.91	0.25	32.0	0.88
	5260	44.9	45.0	179.8	50.5	900	28	–	–	12.49	0.91	0.25	32.0	0.88
	5260	44.9	45.0	179.8	50.5	1200	28	–	–	12.49	0.91	0.25	32.0	0.88
								Mean	1.02				Mean	1.02
								Sd. Dev.	0.11				Sd. Dev.	0.11
								Max	1.40				Max	1.29
								Min	0.73				Min	0.79

ANNEX E: PIN-ENDED COLUMN NUMERICAL DATA

Table E: Pin-ended column numerical ultimate strengths and their estimates according to (i) the proposal of Silvestre *et al.* (2013), and (ii) the developed DSM-P procedure (dimensions in *mm*, stresses in *MPa*)

		Buckling analysis					Numerical	Silvestre *et al.* (2013)		Proposed DSM-P Procedure							
Section	L	f_{crft}	f_{cre}	f_{crf}	f_{crt}	f_y	f_u	f_{nle}	f_u/f_{nle}	Δ_f	a	b	c	d	β	f_{nfte}	f_u/f_{nfte}
70x1.2	532	27.2	1495.6	23922.2	27.3	30	24.2	21.1	1.14	0.04	0.41	0.16	0.61	0.67	1.00	24.2	1.00
	980	24.7	440.8	7049.7	24.8	30	22.6	19.4	1.16	0.13	0.43	0.18	0.61	0.67	1.00	22.4	1.01
	1330	24.2	239.3	3827.5	24.3	30	23.3	18.9	1.23	0.24	0.46	0.20	0.47	0.81	1.00	21.2	1.10
	1820	23.9	127.8	2044.0	24.0	30	20.7	18.3	1.13	0.44	0.50	0.23	0.44	0.83	1.00	19.8	1.05
	2520	23.7	66.7	1066.2	23.9	30	18.7	17.3	1.08	0.85	0.57	0.23	0.39	0.86	1.00	18.7	1.00
	3640	23.4	32.0	511.0	23.8	30	15.1	14.7	1.03	1.80	0.71	0.22	0.25	0.93	1.00	17.4	0.87
	4200	23.2	24.0	383.8	23.8	30	13.2	12.6	1.05	2.42	0.78	0.22	0.16	0.98	0.95	15.9	0.83
	532	27.2	1495.6	23922.2	27.3	60	26.9	24.3	1.11	0.04	0.41	0.16	0.61	0.67	0.86	31.8	0.85
	980	24.7	440.8	7049.7	24.8	60	24	22.0	1.09	0.13	0.43	0.18	0.61	0.67	0.83	27.7	0.87
	1330	24.2	239.3	3827.5	24.3	60	23.9	21.4	1.12	0.24	0.46	0.20	0.47	0.81	0.72	22.3	1.07
	1820	23.9	127.8	2044.0	24.0	60	21	20.6	1.02	0.44	0.50	0.23	0.44	0.83	0.73	20.2	1.04
	2520	23.7	66.7	1066.2	23.9	60	18.8	19.3	0.97	0.85	0.57	0.23	0.39	0.86	0.76	18.3	1.03
	3640	23.4	32.0	511.0	23.8	60	15.3	15.0	1.02	1.80	0.71	0.22	0.25	0.93	0.83	16.0	0.96
	4200	23.2	24.0	383.8	23.8	60	13.4	12.0	1.12	2.42	0.78	0.22	0.16	0.98	0.86	15.1	0.89
	532	27.2	1495.6	23922.2	27.3	120	29.4	25.9	1.14	0.04	0.41	0.16	0.61	0.67	0.60	33.9	0.87
	980	24.7	440.8	7049.7	24.8	120	25.9	23.3	1.11	0.13	0.43	0.18	0.61	0.67	0.60	29.3	0.88
	1330	24.2	239.3	3827.5	24.3	120	25.5	22.5	1.13	0.24	0.46	0.20	0.47	0.81	0.52	22.6	1.13
	1820	23.9	127.8	2044.0	24.0	120	21	21.7	0.97	0.44	0.50	0.23	0.44	0.83	0.55	20.0	1.05
	2520	23.7	66.7	1066.2	23.9	120	18.8	19.6	0.96	0.85	0.57	0.23	0.39	0.86	0.63	17.7	1.07
	3640	23.4	32.0	511.0	23.8	120	15.3	14.8	1.03	1.80	0.71	0.22	0.25	0.93	0.82	15.9	0.96
	4200	23.2	24.0	383.8	23.8	120	13.4	12.0	1.12	2.42	0.78	0.22	0.16	0.98	0.86	15.1	0.89
	532	27.2	1495.6	23922.2	27.3	235	38.4	26.7	1.44	0.04	0.41	0.16	0.61	0.67	0.45	37.6	1.02
	980	24.7	440.8	7049.7	24.8	235	30.3	23.9	1.27	0.13	0.43	0.18	0.61	0.67	0.46	31.8	0.95
	1330	24.2	239.3	3827.5	24.3	235	25.7	23.1	1.11	0.24	0.46	0.20	0.47	0.81	0.41	23.3	1.10
	1820	23.9	127.8	2044.0	24.0	235	21	21.8	0.96	0.44	0.50	0.23	0.44	0.83	0.47	20.1	1.05
	2520	23.7	66.7	1066.2	23.9	235	18.8	19.5	0.96	0.85	0.57	0.23	0.39	0.86	0.62	17.6	1.07
	3640	23.4	32.0	511.0	23.8	235	15.3	14.8	1.03	1.80	0.71	0.22	0.25	0.93	0.82	15.9	0.96
	4200	23.2	24.0	383.8	23.8	235	13.4	12.0	1.12	2.42	0.78	0.22	0.16	0.98	0.86	15.1	0.89
	532	27.2	1495.6	23922.2	27.3	400	45.2	27.0	1.67	0.04	0.41	0.16	0.61	0.67	0.37	41.4	1.09
	980	24.7	440.8	7049.7	24.8	400	35	24.1	1.17	0.13	0.43	0.18	0.61	0.67	0.40	33.9	1.03
	1330	24.2	239.3	3827.5	24.3	400	27.1	23.1	1.17	0.24	0.46	0.20	0.47	0.81	0.36	23.8	1.14
	1820	23.9	127.8	2044.0	24.0	400	21	21.7	0.97	0.44	0.50	0.23	0.44	0.83	0.46	20.1	1.05
	2520	23.7	66.7	1066.2	23.9	400	18.8	19.5	0.96	0.85	0.57	0.23	0.39	0.86	0.62	17.6	1.07
	3640	23.4	32.0	511.0	23.8	400	15.3	14.8	1.03	1.80	0.71	0.22	0.25	0.93	0.82	15.9	0.96
	4200	23.2	24.0	383.8	23.8	400	13.4	12.0	1.12	2.42	0.78	0.22	0.16	0.98	0.86	15.1	0.89
	532	27.2	1495.6	23922.2	27.3	500	47.1	27.1	1.74	0.04	0.41	0.16	0.61	0.67	0.34	43.1	1.09
	980	24.7	440.8	7049.7	24.8	500	35	24.2	1.17	0.13	0.43	0.18	0.61	0.67	0.38	34.8	1.01
	1330	24.2	239.3	3827.5	24.3	500	27.1	23.1	1.18	0.24	0.46	0.20	0.47	0.81	0.35	23.9	1.14
	1820	23.9	127.8	2044.0	24.0	500	21	21.7	0.97	0.44	0.50	0.23	0.44	0.83	0.46	20.1	1.05
	2520	23.7	66.7	1066.2	23.9	500	18.8	19.5	0.96	0.85	0.57	0.23	0.39	0.86	0.62	17.6	1.07
	3640	23.4	32.0	511.0	23.8	500	15.3	14.8	1.03	1.80	0.71	0.22	0.25	0.93	0.82	15.9	0.96
	4200	23.2	24.0	383.8	23.8	500	13.4	12.0	1.12	2.42	0.78	0.22	0.16	0.98	0.86	15.1	0.89
50x1.2	750	48.1	384.1	6141.1	48.3	120	45.3	42.3	1.07	0.30	0.47	0.21	0.47	0.82	0.72	43.3	1.05
	950	47.4	239.4	3827.5	47.6	120	42.7	40.9	1.05	0.47	0.51	0.23	0.44	0.83	0.73	39.7	1.07
	1500	46.4	96.0	1535.3	47.0	120	40.1	35.8	1.12	1.17	0.62	0.21	0.34	0.88	0.78	34.4	1.16
	2000	45.8	54.0	863.6	46.8	120	36.5	26.4	1.38	2.10	0.75	0.22	0.21	0.96	0.85	30.5	1.20

Section	L	f_{crft}	f_{cre}	f_{crf}	f_{crt}	f_y	f_u	f_{nle}	f_u/f_{nle}	Δ_f	a	b	c	d	β	f_{nfte}	f_u/f_{nfte}
50x1.2	750	48.1	384.1	6141.1	48.3	235	46.5	44.5	1.04	0.30	0.47	0.21	0.47	0.82	0.53	43.5	1.07
	950	47.4	239.4	3827.5	47.6	235	42.7	42.8	1.00	0.47	0.51	0.23	0.44	0.83	0.56	39.2	1.09
	1500	46.4	96.0	1535.3	47.0	235	40.1	35.2	1.14	1.17	0.62	0.21	0.34	0.88	0.71	33.4	1.20
	2000	45.8	54.0	863.6	46.8	235	36.5	26.4	1.38	2.10	0.75	0.22	0.21	0.96	0.85	30.5	1.20
	750	48.1	384.1	6141.1	48.3	400	46.5	45.3	1.03	0.30	0.47	0.21	0.47	0.82	0.44	44.2	1.05
	950	47.4	239.4	3827.5	47.6	400	42.7	43.0	0.99	0.47	0.51	0.23	0.44	0.83	0.49	39.3	1.09
	1500	46.4	96.0	1535.3	47.0	400	40.1	35.2	1.14	1.17	0.62	0.21	0.34	0.88	0.71	33.4	1.20
	2000	45.8	54.0	863.6	46.8	400	36.5	26.4	1.38	2.10	0.75	0.22	0.21	0.96	0.85	30.5	1.20
	750	48.1	384.1	6141.1	48.3	500	46.5	45.4	1.02	0.30	0.47	0.21	0.47	0.82	0.42	44.5	1.05
	950	47.4	239.4	3827.5	47.6	500	42.7	42.8	1.00	0.47	0.51	0.23	0.44	0.83	0.48	39.3	1.09
	1500	46.4	96.0	1535.3	47.0	500	40.1	35.2	1.14	1.17	0.62	0.21	0.34	0.88	0.71	33.4	1.20
	2000	45.8	54.0	863.6	46.8	500	36.5	26.4	1.38	2.10	0.75	0.22	0.21	0.96	0.85	30.5	1.20
50x2.6	750	223.5	385.0	6141.1	226.7	235	182	142.6	1.28	1.42	0.66	0.21	0.30	0.90	1.00	162.2	1.12
	950	218.6	239.9	3827.5	223.6	235	154	119.2	1.29	2.27	0.77	0.22	0.18	0.97	1.00	154.0	1.00
	750	223.5	385.0	6141.1	226.7	400	189	159.8	1.18	1.42	0.66	0.21	0.30	0.90	0.89	167.0	1.13
	950	218.6	239.9	3827.5	223.6	400	164	123.8	1.32	2.27	0.77	0.22	0.18	0.97	0.89	146.6	1.12
	750	223.5	385.0	6141.1	226.7	500	189	162.5	1.16	1.42	0.66	0.21	0.30	0.90	0.83	162.7	1.16
	950	218.6	239.9	3827.5	223.6	500	164	120.0	1.37	2.27	0.77	0.22	0.18	0.97	0.86	144.5	1.13
90x2.5	1000	66.5	700.1	11192.1	66.6	120	62.3	–	–	0.22	0.45	0.20	0.48	0.81	0.86	62.5	1.00
	1000	66.5	700.1	11192.1	66.6	235	65.1	–	–	0.22	0.45	0.20	0.48	0.81	0.60	62.2	1.05
	1000	66.5	700.1	11192.1	66.6	400	68.6	–	–	0.22	0.45	0.20	0.48	0.81	0.48	63.4	1.08
	1000	66.5	700.1	11192.1	66.6	500	69.7	–	–	0.22	0.45	0.20	0.48	0.81	0.44	64.1	1.09
	1000	66.5	700.1	11192.1	66.6	600	69.9	–	–	0.22	0.45	0.20	0.48	0.81	0.41	64.7	1.08
	1000	66.5	700.1	11192.1	66.6	900	69.9	–	–	0.22	0.45	0.20	0.48	0.81	0.37	65.9	1.06
	1000	66.5	700.1	11192.1	66.6	1200	69.9	–	–	0.22	0.45	0.20	0.48	0.81	0.35	66.6	1.05
	1200	65.1	486.2	7772.3	65.3	120	60.3	–	–	0.32	0.48	0.22	0.46	0.82	0.86	58.7	1.03
	1200	65.1	486.2	7772.3	65.3	235	62.2	–	–	0.32	0.48	0.22	0.46	0.82	0.61	57.9	1.07
	1200	65.1	486.2	7772.3	65.3	400	63	–	–	0.32	0.48	0.22	0.46	0.82	0.49	58.5	1.08
	1200	65.1	486.2	7772.3	65.3	500	63	–	–	0.32	0.48	0.22	0.46	0.82	0.46	58.8	1.07
	1200	65.1	486.2	7772.3	65.3	600	63	–	–	0.32	0.48	0.22	0.46	0.82	0.44	59.1	1.07
	1200	65.1	486.2	7772.3	65.3	900	63	–	–	0.32	0.48	0.22	0.46	0.82	0.40	59.6	1.06
	1200	65.1	486.2	7772.3	65.3	1200	63	–	–	0.32	0.48	0.22	0.46	0.82	0.40	59.7	1.06
	1500	63.9	311.2	4974.3	64.2	120	57.7	–	–	0.49	0.51	0.23	0.44	0.83	0.85	54.2	1.06
	1500	63.9	311.2	4974.3	64.2	235	57.9	–	–	0.49	0.51	0.23	0.44	0.83	0.62	52.8	1.10
	1500	63.9	311.2	4974.3	64.2	400	57.9	–	–	0.49	0.51	0.23	0.44	0.83	0.53	52.5	1.10
	1500	63.9	311.2	4974.3	64.2	500	57.9	–	–	0.49	0.51	0.23	0.44	0.83	0.50	52.5	1.10
	1500	63.9	311.2	4974.3	64.2	600	57.9	–	–	0.49	0.51	0.23	0.44	0.83	0.49	52.6	1.10
	1500	63.9	311.2	4974.3	64.2	900	57.9	–	–	0.49	0.51	0.23	0.44	0.83	0.48	52.6	1.10
	1500	63.9	311.2	4974.3	64.2	1200	57.9	–	–	0.49	0.51	0.23	0.44	0.83	0.48	52.6	1.10
	2000	62.9	175.0	2798.0	63.4	120	53.4	–	–	0.86	0.58	0.23	0.38	0.86	0.86	49.8	1.07
	2000	62.9	175.0	2798.0	63.4	235	53.4	–	–	0.86	0.58	0.23	0.38	0.86	0.67	47.3	1.13
	2000	62.9	175.0	2798.0	63.4	400	53.4	–	–	0.86	0.58	0.23	0.38	0.86	0.62	46.7	1.14
	2000	62.9	175.0	2798.0	63.4	500	53.4	–	–	0.86	0.58	0.23	0.38	0.86	0.62	46.7	1.14
	2000	62.9	175.0	2798.0	63.4	600	53.4	–	–	0.86	0.58	0.23	0.38	0.86	0.62	46.7	1.14
	2000	62.9	175.0	2798.0	63.4	900	53.4	–	–	0.86	0.58	0.23	0.38	0.86	0.62	46.7	1.14
	2000	62.9	175.0	2798.0	63.4	1200	53.4	–	–	0.86	0.58	0.23	0.38	0.86	0.62	46.7	1.14
	2500	62.2	112.0	1790.7	63.0	120	48.9	–	–	1.35	0.65	0.21	0.31	0.90	0.87	46.3	1.06
	2500	62.2	112.0	1790.7	63.0	235	48.9	–	–	1.35	0.65	0.21	0.31	0.90	0.75	44.0	1.11
	2500	62.2	112.0	1790.7	63.0	400	48.9	–	–	1.35	0.65	0.21	0.31	0.90	0.75	44.0	1.11
	2500	62.2	112.0	1790.7	63.0	500	48.9	–	–	1.35	0.65	0.21	0.31	0.90	0.75	44.0	1.11
	2500	62.2	112.0	1790.7	63.0	600	48.9	–	–	1.35	0.65	0.21	0.31	0.90	0.75	44.0	1.11
	2500	62.2	112.0	1790.7	63.0	900	48.9	–	–	1.35	0.65	0.21	0.31	0.90	0.75	44.0	1.11
	2500	62.2	112.0	1790.7	63.0	1200	48.9	–	–	1.35	0.65	0.21	0.31	0.90	0.75	44.0	1.11

Section	L	f_{crft}	f_{cre}	f_{crf}	f_{crt}	f_y	f_u	f_{nle}	f_u/f_{nle}	Δ_f	a	b	c	d	β	f_{nfte}	f_u/f_{nfte}
	3000	61.6	77.8	1243.6	62.8	120	43.6	–	–	1.95	0.73	0.22	0.23	0.95	0.88	42.4	1.03
	3000	61.6	77.8	1243.6	62.8	235	43.6	–	–	1.95	0.73	0.22	0.23	0.95	0.83	41.5	1.05
	3000	61.6	77.8	1243.6	62.8	400	43.6	–	–	1.95	0.73	0.22	0.23	0.95	0.83	41.5	1.05
90x2.5	3000	61.6	77.8	1243.6	62.8	500	43.6	–	–	1.95	0.73	0.22	0.23	0.95	0.83	41.5	1.05
	3000	61.6	77.8	1243.6	62.8	600	43.6	–	–	1.95	0.73	0.22	0.23	0.95	0.83	41.5	1.05
	3000	61.6	77.8	1243.6	62.8	900	43.6	–	–	1.95	0.73	0.22	0.23	0.95	0.83	41.5	1.05
	3000	61.6	77.8	1243.6	62.8	1200	43.6	–	–	1.95	0.73	0.22	0.23	0.95	0.83	41.5	1.05
	700	71.4	864.4	13817.4	71.6	120	66.8	–	–	0.19	0.45	0.20	0.49	0.80	0.91	69.4	0.96
	700	71.4	864.4	13817.4	71.6	235	70.1	–	–	0.19	0.45	0.20	0.49	0.80	0.63	69.0	1.02
	700	71.4	864.4	13817.4	71.6	400	74.5	–	–	0.19	0.45	0.20	0.49	0.80	0.49	70.7	1.05
	700	71.4	864.4	13817.4	71.6	500	76.9	–	–	0.19	0.45	0.20	0.49	0.80	0.45	71.6	1.07
	700	71.4	864.4	13817.4	71.6	600	78.4	–	–	0.19	0.45	0.20	0.49	0.80	0.42	72.4	1.08
	700	71.4	864.4	13817.4	71.6	900	79.1	–	–	0.19	0.45	0.20	0.49	0.80	0.37	74.3	1.07
	700	71.4	864.4	13817.4	71.6	1200	79.1	–	–	0.19	0.45	0.20	0.49	0.80	0.35	75.4	1.05
	800	70.1	661.8	10579.0	70.3	120	65.2	–	–	0.25	0.46	0.21	0.47	0.81	0.89	65.3	1.00
	800	70.1	661.8	10579.0	70.3	235	67.9	–	–	0.25	0.46	0.21	0.47	0.81	0.62	64.6	1.05
	800	70.1	661.8	10579.0	70.3	400	70.9	–	–	0.25	0.46	0.21	0.47	0.81	0.49	65.6	1.08
	800	70.1	661.8	10579.0	70.3	500	71.7	–	–	0.25	0.46	0.21	0.47	0.81	0.45	66.2	1.08
	800	70.1	661.8	10579.0	70.3	600	71.7	–	–	0.25	0.46	0.21	0.47	0.81	0.43	66.7	1.08
	800	70.1	661.8	10579.0	70.3	900	71.7	–	–	0.25	0.46	0.21	0.47	0.81	0.38	67.8	1.06
	800	70.1	661.8	10579.0	70.3	1200	71.7	–	–	0.25	0.46	0.21	0.47	0.81	0.36	68.3	1.05
70x2.0	900	69.1	522.9	8358.7	69.3	120	63.8	–	–	0.31	0.47	0.22	0.46	0.82	0.89	62.7	1.02
	900	69.1	522.9	8358.7	69.3	235	66	–	–	0.31	0.47	0.22	0.46	0.82	0.62	61.6	1.07
	900	69.1	522.9	8358.7	69.3	400	67.2	–	–	0.31	0.47	0.22	0.46	0.82	0.50	62.2	1.08
	900	69.1	522.9	8358.7	69.3	500	67.2	–	–	0.31	0.47	0.22	0.46	0.82	0.47	62.6	1.07
	900	69.1	522.9	8358.7	69.3	600	67.2	–	–	0.31	0.47	0.22	0.46	0.82	0.44	62.9	1.07
	900	69.1	522.9	8358.7	69.3	900	67.2	–	–	0.31	0.47	0.22	0.46	0.82	0.41	63.5	1.06
	900	69.1	522.9	8358.7	69.3	1200	67.2	–	–	0.31	0.47	0.22	0.46	0.82	0.40	63.7	1.06
	1000	68.4	423.5	6770.5	68.7	120	62.7	–	–	0.38	0.49	0.22	0.45	0.82	0.88	60.3	1.04
	1000	68.4	423.5	6770.5	68.7	235	64	–	–	0.38	0.49	0.22	0.45	0.82	0.63	58.9	1.09
	1000	68.4	423.5	6770.5	68.7	400	64.3	–	–	0.38	0.49	0.22	0.45	0.82	0.51	59.1	1.09
	1000	68.4	423.5	6770.5	68.7	500	64.3	–	–	0.38	0.49	0.22	0.45	0.82	0.48	59.2	1.09
	1000	68.4	423.5	6770.5	68.7	600	64.3	–	–	0.38	0.49	0.22	0.45	0.82	0.46	59.4	1.08
	1000	68.4	423.5	6770.5	68.7	900	64.3	–	–	0.38	0.49	0.22	0.45	0.82	0.44	59.6	1.08
	1000	68.4	423.5	6770.5	68.7	1200	64.3	–	–	0.38	0.49	0.22	0.45	0.82	0.43	59.6	1.08
	1500	66.6	188.2	3009.1	67.2	120	56.8	–	–	0.85	0.57	0.23	0.39	0.86	0.88	53.1	1.07
	1500	66.6	188.2	3009.1	67.2	235	56.8	–	–	0.85	0.57	0.23	0.39	0.86	0.68	50.3	1.13
	1500	66.6	188.2	3009.1	67.2	400	56.8	–	–	0.85	0.57	0.23	0.39	0.86	0.62	49.5	1.15
	1500	66.6	188.2	3009.1	67.2	500	56.8	–	–	0.85	0.57	0.23	0.39	0.86	0.62	49.5	1.15
	1500	66.6	188.2	3009.1	67.2	600	56.8	–	–	0.85	0.57	0.23	0.39	0.86	0.62	49.5	1.15
	1500	66.6	188.2	3009.1	67.2	900	56.8	–	–	0.85	0.57	0.23	0.39	0.86	0.62	49.5	1.15
	1500	66.6	188.2	3009.1	67.2	1200	56.8	–	–	0.85	0.57	0.23	0.39	0.86	0.62	49.5	1.15
	2000	65.6	105.9	1692.6	66.6	120	50.5	–	–	1.51	0.67	0.22	0.29	0.91	0.89	48.1	1.05
	2000	65.6	105.9	1692.6	66.6	235	50.5	–	–	1.51	0.67	0.22	0.29	0.91	0.78	45.7	1.11
	2000	65.6	105.9	1692.6	66.6	400	50.5	–	–	1.51	0.67	0.22	0.29	0.91	0.78	45.7	1.11
	2000	65.6	105.9	1692.6	66.6	500	50.5	–	–	1.51	0.67	0.22	0.29	0.91	0.78	45.7	1.11
	2000	65.6	105.9	1692.6	66.6	600	50.5	–	–	1.51	0.67	0.22	0.29	0.91	0.78	45.7	1.11
	2000	65.6	105.9	1692.6	66.6	900	50.5	–	–	1.51	0.67	0.22	0.29	0.91	0.78	45.7	1.11
	2000	65.6	105.9	1692.6	66.6	1200	50.5	–	–	1.51	0.67	0.22	0.29	0.91	0.78	45.7	1.11

Section	L	f_{crft}	f_{cre}	f_{crf}	f_{crt}	f_y	f_u	f_{nle}	f_u/f_{nle}	Δ_f	a	b	c	d	β	f_{nfte}	f_u/f_{nfte}
	2500	64.8	67.8	1083.3	66.4	120	42.7	–	–	2.39	0.78	0.22	0.17	0.98	0.88	42.8	1.00
	2500	64.8	67.8	1083.3	66.4	235	42.7	–	–	2.39	0.78	0.22	0.17	0.98	0.86	42.3	1.01
	2500	64.8	67.8	1083.3	66.4	400	42.7	–	–	2.39	0.78	0.22	0.17	0.98	0.86	42.3	1.01
70x2.0	2500	64.8	67.8	1083.3	66.4	500	42.7	–	–	2.39	0.78	0.22	0.17	0.98	0.86	42.3	1.01
	2500	64.8	67.8	1083.3	66.4	600	42.7	–	–	2.39	0.78	0.22	0.17	0.98	0.86	42.3	1.01
	2500	64.8	67.8	1083.3	66.4	900	42.7	–	–	2.39	0.78	0.22	0.17	0.98	0.86	42.3	1.01
	2500	64.8	67.8	1083.3	66.4	1200	42.7	–	–	2.39	0.78	0.22	0.17	0.98	0.86	42.3	1.01
	800	52.8	486.1	7772.3	52.9	120	49.8	–	–	0.26	0.46	0.21	0.47	0.81	0.76	48.4	1.03
	800	52.8	486.1	7772.3	52.9	235	52.1	–	–	0.26	0.46	0.21	0.47	0.81	0.55	48.7	1.07
	800	52.8	486.1	7772.3	52.9	400	52.8	–	–	0.26	0.46	0.21	0.47	0.81	0.44	49.6	1.06
	800	52.8	486.1	7772.3	52.9	500	52.8	–	–	0.26	0.46	0.21	0.47	0.81	0.41	50.1	1.05
	800	52.8	486.1	7772.3	52.9	600	52.8	–	–	0.26	0.46	0.21	0.47	0.81	0.40	50.5	1.05
	800	52.8	486.1	7772.3	52.9	900	52.8	–	–	0.26	0.46	0.21	0.47	0.81	0.37	51.0	1.03
	800	52.8	486.1	7772.3	52.9	1200	52.8	–	–	0.26	0.46	0.21	0.47	0.81	0.36	51.2	1.03
	900	52.2	384.1	6141.1	52.4	120	48.7	–	–	0.32	0.48	0.22	0.46	0.82	0.76	46.5	1.05
	900	52.2	384.1	6141.1	52.4	235	49.9	–	–	0.32	0.48	0.22	0.46	0.82	0.55	46.4	1.08
	900	52.2	384.1	6141.1	52.4	400	50	–	–	0.32	0.48	0.22	0.46	0.82	0.46	47.0	1.06
	900	52.2	384.1	6141.1	52.4	500	50	–	–	0.32	0.48	0.22	0.46	0.82	0.43	47.2	1.06
	900	52.2	384.1	6141.1	52.4	600	50	–	–	0.32	0.48	0.22	0.46	0.82	0.42	47.4	1.05
	900	52.2	384.1	6141.1	52.4	900	50	–	–	0.32	0.48	0.22	0.46	0.82	0.40	47.6	1.05
	900	52.2	384.1	6141.1	52.4	1200	50	–	–	0.32	0.48	0.22	0.46	0.82	0.40	47.6	1.05
60x1.5	1000	51.8	311.1	4974.3	52.0	120	43.8	–	–	0.39	0.49	0.23	0.45	0.83	0.76	44.8	0.98
	1000	51.8	311.1	4974.3	52.0	235	43.9	–	–	0.39	0.49	0.23	0.45	0.83	0.56	44.3	0.99
	1000	51.8	311.1	4974.3	52.0	400	43.9	–	–	0.39	0.49	0.23	0.45	0.83	0.48	44.6	0.99
	1000	51.8	311.1	4974.3	52.0	500	43.9	–	–	0.39	0.49	0.23	0.45	0.83	0.46	44.7	0.98
	1000	51.8	311.1	4974.3	52.0	600	43.9	–	–	0.39	0.49	0.23	0.45	0.83	0.44	44.7	0.98
	1000	51.8	311.1	4974.3	52.0	900	43.9	–	–	0.39	0.49	0.23	0.45	0.83	0.44	44.8	0.98
	1000	51.8	311.1	4974.3	52.0	1200	43.9	–	–	0.39	0.49	0.23	0.45	0.83	0.44	44.8	0.98
	1500	50.7	138.3	2210.8	51.2	120	42.5	–	–	0.88	0.58	0.23	0.38	0.86	0.79	39.3	1.08
	1500	50.7	138.3	2210.8	51.2	235	42.5	–	–	0.88	0.58	0.23	0.38	0.86	0.65	37.8	1.12
	1500	50.7	138.3	2210.8	51.2	400	42.5	–	–	0.88	0.58	0.23	0.38	0.86	0.63	37.6	1.13
	1500	50.7	138.3	2210.8	51.2	500	42.5	–	–	0.88	0.58	0.23	0.38	0.86	0.63	37.6	1.13
	1500	50.7	138.3	2210.8	51.2	600	42.5	–	–	0.88	0.58	0.23	0.38	0.86	0.63	37.6	1.13
	1500	50.7	138.3	2210.8	51.2	900	42.5	–	–	0.88	0.58	0.23	0.38	0.86	0.63	37.6	1.13
	1500	50.7	138.3	2210.8	51.2	1200	42.5	–	–	0.88	0.58	0.23	0.38	0.86	0.63	37.6	1.13
	2000	50.1	77.8	1243.6	50.9	120	37.2	–	–	1.57	0.68	0.22	0.28	0.92	0.83	35.3	1.05
	2000	50.1	77.8	1243.6	50.9	235	37.2	–	–	1.57	0.68	0.22	0.28	0.92	0.79	34.7	1.07
	2000	50.1	77.8	1243.6	50.9	400	37.2	–	–	1.57	0.68	0.22	0.28	0.92	0.79	34.7	1.07
	2000	50.1	77.8	1243.6	50.9	500	37.2	–	–	1.57	0.68	0.22	0.28	0.92	0.79	34.7	1.07
	2000	50.1	77.8	1243.6	50.9	600	37.2	–	–	1.57	0.68	0.22	0.28	0.92	0.79	34.7	1.07
	2000	50.1	77.8	1243.6	50.9	900	37.2	–	–	1.57	0.68	0.22	0.28	0.92	0.79	34.7	1.07
	2000	50.1	77.8	1243.6	50.9	1200	37.2	–	–	1.57	0.68	0.22	0.28	0.92	0.79	34.7	1.07
	2500	49.5	49.8	795.9	50.7	120	31	–	–	2.49	0.79	0.22	0.15	0.99	0.86	32.0	0.97
	2500	49.5	49.8	795.9	50.7	235	31	–	–	2.49	0.79	0.22	0.15	0.99	0.86	32.0	0.97
	2500	49.5	49.8	795.9	50.7	400	31	–	–	2.49	0.79	0.22	0.15	0.99	0.86	32.0	0.97
	2500	49.5	49.8	795.9	50.7	500	31	–	–	2.49	0.79	0.22	0.15	0.99	0.86	32.0	0.97
	2500	49.5	49.8	795.9	50.7	600	31	–	–	2.49	0.79	0.22	0.15	0.99	0.86	32.0	0.97
	2500	49.5	49.8	795.9	50.7	900	31	–	–	2.49	0.79	0.22	0.15	0.99	0.86	32.0	0.97
	2500	49.5	49.8	795.9	50.7	1200	31	–	–	2.49	0.79	0.22	0.15	0.99	0.86	32.0	0.97
								Mean	1.10							Mean	1.06
								Sd. Dev.	0.11							Sd. Dev.	0.07
								Max	1.74							Max	1.20
								Min	0.96							Min	0.83